Electronic Supplementary Material (ESI) for Physical Chemistry Chemical Physics.

Strong response of Pt clusters to the environment and conditions, formation of metastable states, and simple methods to trace the reversible changes

Alexander S. Lisitsyn and Anastasiya S. Kadtsyna

Boreskov Institute of Catalysis SB RAS, Novosibirsk 630090, Russian Federation

Electronic supplementary information

S1. Experimental details for preconditioning the samples to experiments

In the present study we used 0.5%Pt/γ-Al_2O_3 and 2.5%Pt/γ-Al_2O_3 samples that remained in sufficient quantity after our previous works.[S1,S2] The samples were stored in unreduced form. After placing a sample with supported H_2PtCl_6 into U-type quartz tube (400 mg in the case of 0.5%Pt/γ-Al_2O_3, 200 mg for 2.5%Pt/γ-Al_2O_3) the tube was attached to the instrument, and the sample was heated in a flow of pure O_2 to 500 °C (T_{OX}; 10 °C/min; 1 h at the final temperature). This ensured complete removal of organic substances that could be present after handling the sample in air; simultaneously, the calcination allowed the metal precursor to be uniformly distributed over the support as monoatomic Pt species. The sample was then cooled under O_2 and purged at ambient temperature with He. A flow of pure H_2 was then provided, and the sample was heated in flowing H_2 to the reduction temperature (typically, 400 ºC, 10 °C/min, plus 1 h at the final temperature). The flow was then switched to an inert gas (Ar or He, depending on the case), the temperature was ramped to 500 °C, and the sample was degassed at T_{DEG} of 500 ºC for 20-30 min.

S2. Standard procedures in and between successive runs

(1) After CO chemisorption measurements and experiments on H_2-by-CO displacement: H_2, RT→400 °C (hydrogenation of adsorbed CO); He, 400 °C, 5 min; He, 400→500 °C; He, 500 °C, 10 min; He, 500→T_{TR} (if a new experiment with H_2 treatment was intended); H_2, at T_{TR}, 15 min; H_2, T_{TR}→RT; He (RT), 10 min; +CO (new experiment).

(2) During and between CO-TPD runs: CO dosing (RT); He (RT), 10 min; He, 30→500 °C, 50 °C/min (TPD run); short-time cooling in He; H_2, to 400 °C (hydrogenation of residual CO); He, 400 °C, 5 min; He, 400→500 °C; He, 500 °C, 10 min; He, 500→T_{TR} (if repeated H_2 treatment was intended); H_2, T_{TR}, 15 min; H_2, T_{TR}→RT; He (RT), 10 min; +CO (new experiment).

(3) During and between TPO runs: CO treatment (a flow of 5%CO/He for 10 min); He (RT), 10 min; 5%O_2/He (RT), 10 min; 5%O_2/He, 30→300 °C, 25 °C/min (TPO run); short-time cooling in He; H_2, to 400 °C; He, 400 °C, 5 min; He, 400→500 °C; He, 500 °C, 10 min; He, 500→T_{TR} (if repeated H_2 treatment was intended); H_2, T_{TR}, 15 min; H_2, T_{TR}→RT; He (RT), 10 min; +CO (new experiment).

If not specified otherwise in the protocols, heating rates were 25 °C/min (nominally) and flow rates 25 cc/min, for all gases and gaseous mixtures, both for treatments and purging. In the text above, semicolons separate consecutive steps, RT stays for room temperature and T_{TR} for a certain treatment temperature. The sample was left overnight under a slow flow of inert gas and the experiments continued next day, starting from H_2 retreatment and degassing (H_2, RT→400 °C; He, 400→500 °C).

S3. Control of purity

The methods used for contamination estimates were the same as in our previous works and their detailed description can be found in ref. S1. Small concentrations of O_2 in inert gases were usually estimated *via* treating Pt/γ-Al_2O_3 in flowing gas for different times and measuring the changes in apparent adsorption capacity to O_2 or H_2. The ΔOC and ΔHC values so obtained correspond to the additional quantity of O_2 that came with the carrier gas into the sample zone for the additional time, Δ*t*, and became adsorbed (note that ΔHC = –2ΔOC). This allowed a quality-control check at any time during a series of experiments with a sample, without uninstalling the sample tube or redesigning the connections. One may see example of such tests in Fig. S1. The results were always consistent with those that were obtained with the aid of color-altering O_2 scavengers.[S1] Note that the [O_2] value so obtained includes all O_2 that appeared in the gas, through any leaks, on the way to the sample.

Purity of our gases was >99.999%, before entering the system, and special measures were taken to minimize *diffusion* of air oxygen through nonmetallic components of the instrument, such as sealing rings.[S1] As a result, the concentration of O_2 in the carrier gases was reduced to 1-2 ppm, as measured *in the sample zone*. In these conditions, it takes more than 10-20 h for O_2 impurities to cover all Pt surface, depending on Pt loading and sample mass. We started chemisorption measurements and TPD runs *ca.* 15 and, accordingly, 30 min after sample degassing (the times sufficient for cooling the sample and clamshell furnace, respectively), and the minute traces of oxygen could not violate the results. Confirmation was obtained for all types of experiments (chemisorption, H_2-by-CO displacement, and TPD). Demonstrative examples are provided in Fig. S2 and S3.

The results of those tests simultaneously argue against significant effects of H_2O impurities on adsorption/desorption properties. In comparison to O_2, water molecules diffused more

readily into the gas lines, and the concentration of water vapors in the gas phase was larger than [O_2], yet still sufficiently small (5-15 ppm, as detected in the sample zone, using an empty tube). The presence of water vapors in such amounts was beneficial for our purposes, as it helped to maintain the degree of hydroxylation of alumina surface during the successive runs at (nearly) constant level.

For estimating the amount of carbonaceous deposits on a sample, we applied routine tests using O_2-annealing and measuring the amount of CO_2 formed.[S1] The tests showed that the cleaning procedures used, both before starting the experimental session and between the consecutive runs, effectively eliminate all carbon-containing species. Figure S4 shows the results of another test, confirming the basic ones.

S4. Details of data treatment and presentation

The adsorption/desorption processes were monitored by using TCD and MS. Preference was given to TCD due to its constant sensitivity and good linearity (signal intensity *vs*. probe volume). Examples of calibration plots for H_2 in Ar are provided in Fig. S5. The Table below lists relative sensitivities to H_2, CO, and CO_2, as found experimentally from the slopes of *S*-*vs*-*V* plots (as in Fig. S5, lower panel). When repeated in different times but under identical conditions, TCD calibrations matched each other. During a series of experiments, the detector sensitivity was routinely checked by dosing a 10H_2/Ar or 10%CO/He mixture from the loop and measuring the area of resulting peak, S_d (as in H_2 or CO chemisorption measurements but in bypass to the sample tube). This was done daily. The S_d values could vary, within 5 rel% utmost, due to varying ambient conditions (*P* and *T*, which slightly influence the probe volume and flow rate of carrier gas). When necessary, correction was made.

TCD calibration data (molar sensitivity to H_2 in Ar was taken for unity).

	H_2	CO	CO_2
Ar as the carrier gas	1	0.08	0.04
He as the carrier gas	~0.04*	1.50	1.75

*Rough value, corresponding to the case of low H_2 concentrations in He.

Calibration of mass spectrometer to CO and CO_2 was made analogously, and the results obtained with MS and TCD were in close agreement (see Fig. S6). As compared to TCD, the sensitivity of MS was less constant and needed more attention; besides, quantitative measurements for H_2 were not possible in this case.

Following each experimental run (chemisorption, TPD, or TPO), the carrier gas was directed to the detector(s) in bypass to sample tube. This allowed to check the background level and to subtract the baseline correctly. Aside from the subtraction of baseline, the curves in all figures are presented as recorded in experiments, without smoothing or averaging.

The amount of CO consumed during CO pulse chemisorption was calculated by formula: $V_a = V_d(N - \Sigma S_i/S_d)$ μmol, where V_d is the amount of CO per pulse, N the number of injections, S_i the area under i^{th} peak, and S_d the area corresponding to the dose at zero consumption. The latter value was found in the same experiment, by injecting the dose into the carrier gas bypassing the sample tube. Supplementary data in Fig. S7-S9 confirm that all samples fully consume the first doses of CO, are rapidly saturated by a few doses, and no further adsorption takes place in these conditions if additional doses of CO are provided. Using helium as the carrier gas leads to a strong decrease of TCD sensitivity towards H_2, and evolving H_2 does not seriously affect the measurements for heavy gases, such as CO. The tiny peaks that are detectable by TCD after the first one-two doses of CO to H_2-pretreated Pt/γ-Al_2O_3 relate exclusively to evolving H_2. It may seem surprising that the hydrogen peaks in Fig. 1a in the main text, as well as in Fig. S7 and S8, have the same polarity as CO peaks, but such an effect is well known for low-concentrated H_2-in-He mixtures.[S3,S4]

No methane formation took place during CO chemisorption (Fig. S9), and traces of methane were only detected during CO TPD (in amounts ≤ 1 % of CO). The absence of other products apart from CO, CO_2, and H_2 made it possible to monitor the desorption process using TCD, by tuning it to H_2 (Ar as the carrier gas) or to CO (by using He as the carrier gas and trapping CO_2 at 77 K). In the latter case, CO TPD run was followed by measuring the amount of CO_2 accumulated in the trap.

The high heating rate in TPD experiments, 50 °C/min, was provided for the purpose of enhancing the desorption rate and, so, the concentration of desorbed species in the carrier gas (signal-to-noise ratio). This allowed reliable monitoring of the desorption process even at low Pt loading. In the experiments on temperature-programmed oxidation, it was possible to

provide slower heating, and CO_{ads}-TPO runs were performed at nominal heating rate of 25 °C/min.

Heating was controlled by a thermocouple embedded in the furnace, and real temperature, T_{exp}, was measured by thermocouple in the middle of sample. As the temperature regime in all TPD experiments, as well as in all TPO runs, was the same, T_{exp}-*vs*-*t* curves were also very similar; some difference could only originate from non-identical positions of thermocouple inside the sample. Therefore, we preferred to use predetermined *T*-*vs*-*t* plots and insert thermocouple outside the sample tube, thereby preventing any interference from the thermocouple on results.

In view of the temperature lag at the beginning of heating and because heating was followed by an isothermal hold, TPD curves in all figures are presented as a concentration-*vs*-time plots, with a liner scale for the concentration and time. In this case, the area under a curve at a time *t* is directly proportional to the volume of a gas that has been desorbed and reached the detector by that time.

For convenience, we provide Fig. S10–S12, which are the same as Fig. 4, 5, and 7 in the main text but include *T*-vs-*t* plots for those experiments. It was taken into account that the gas mixture living the sample tube needs some time to arrive at the detector (0.5-1 min in our case, if the trap is used and depending on the temperature of the trap). Therefore, at a time *t*, the detector "sees" events that took place a little bit earlier, when the sample temperature was lower than T_{exp} at the time *t*. Solid purple lines in Fig. S10-S12 show T_{exp}-vs-*t* curves as recorded in the experiments, while dashed purple curves show temperatures *T** that truly correspond to TCD response, *i.e.*, with account for the time lag between the sample reaction and TCD response.

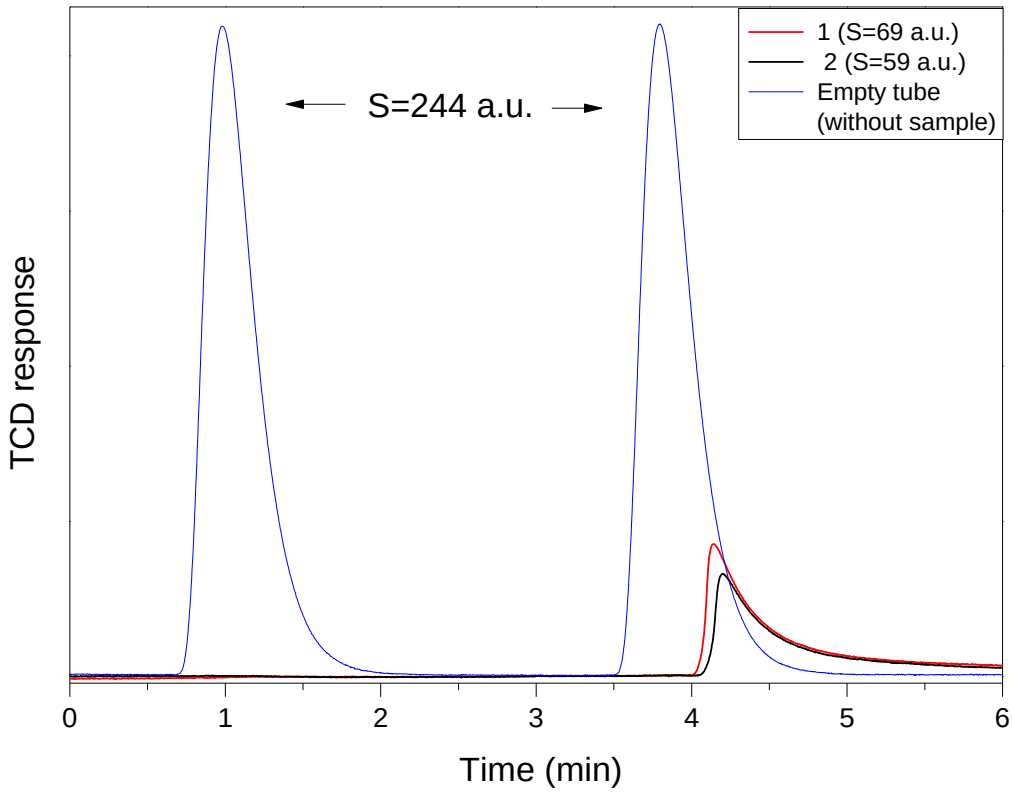

Fig. S1. Estimating the amount of O_2 impurities in the carrier gas with the aid of H_2 chemisorption (HC). In case 1, 0.5%Pt/Al_2O_3 sample was degassed in Ar under standard conditions (500 °C, 10 min), then cooled to room temperature (for 10 min; total time in Ar 20 min), and finally treated by two 72-µl doses of H_2. In case 2 (black curve), pretreatments were the same as before, but the sample was additionally kept under Ar for 30 min before H_2 dosing; total time in Ar 50 min. The difference in the areas under the red and black curves corresponds to the extra amount of H_2 that was consumed due to the reaction with adsorbed oxygen (accumulated for 50-20=30 min). The difference only equals to ~2% of the H_2 adsorbed.

Note that under the conditions in this figure the sample fully consumes the first dose of H_2. If it was left under the Ar flow for much longer time, ~20 h, or intentionally dosed with O_2, by pulsing, it consumed almost three such doses of H_2.

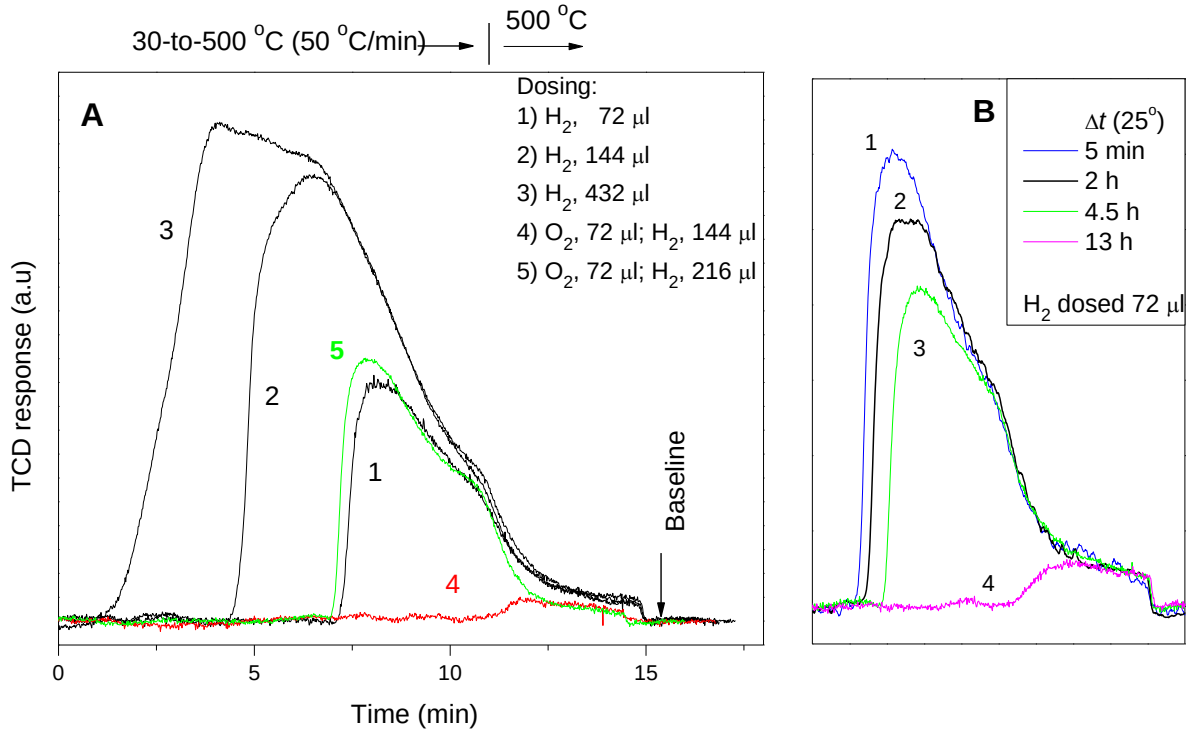

Fig. S2. An extended series of experiments on estimating the degree of Pt oxidation by O_2 traces in the carrier gas. **A**: H_2 TPD from 2.5%Pt/γ-Al_2O_3 (200 mg) after treating the sample by varying amounts of H_2 and O_2; **B**: changes in H_2-TPD trace with the time of sample exposure to the carrier gas. Before each of the runs, the sample was degassed in Ar at 500 °C for 10 min, and H_2/O_2 injections were made at room temperature. Further details are provided in the figure and in the attached Table.

Curves 1-3 in panel A indicate that the amount of H_2 in one 72-µl pulse is sufficiently small to be fully retained by the sample, and the hydrogen desorbs only at a high temperature. Therefore, a decrease in the curve area can only be expected form side processes, such as reaction of H_2 with adsorbed oxygen. When a 72-µl dose of O_2 is provided to the sample, the adsorbed oxygen consumes two further doses of H_2 (case 4 in A), but three doses of H_2 result in curve 5, which area equals to that in run 1, as expected. The absence of H_2 evolution during run 4 simultaneously indicates that oxidation of Pt by H_2O, which was formed through the O_2+H_2 reaction, does not take place.

In case 1 in B, the duration of pretreatments was reduced to minimum (H_2 was dosed 5 min after sample degassing). The area under curve 1 in B is somewhat smaller than expected for the 72-µl dose of H_2 (in this series, S_0 = 243 ±3 units), but this is mainly due to the strong retention of residual hydrogen by the sample (the hydrogen still evolves at the end of the runs). By comparing curves 1-4 in B and corresponding *S* values in the attached Table, one can see that it takes half a day for O_2 impurities to be accumulated in amounts sufficient to react with all H_2 in the dose, making H_2 desorption barely visible (curve 4 in B).

When the pretreatments were performed in He, instead of Ar, the results were similar to those presented above.

Experimental details to Figure S2:

	Predosing (STP values)	Δt*	Curve area S (a.u)
A			
1	H_2, 72 µl	35 min	178
2	H_2, 2×72 µl	35 min	447
3	H_2, 6×72 µl (in excess)	45 min	693
4	O_2, 72 µl, then H_2, 2×72 µl	40 min	~0
5	O_2, 72 µl, then H_2, 3×72 µl	40 min	180
B			
1	H_2, 72 µl	5 min	198
2	H_2, 72 µl	2 h	181
3	H_2, 72 µl	4.5 h	144
4	H_2, 72 µl	13 h (overnight)	16

* Holding time in the carrier gas after degassing (before dosing H_2 and starting TPD).

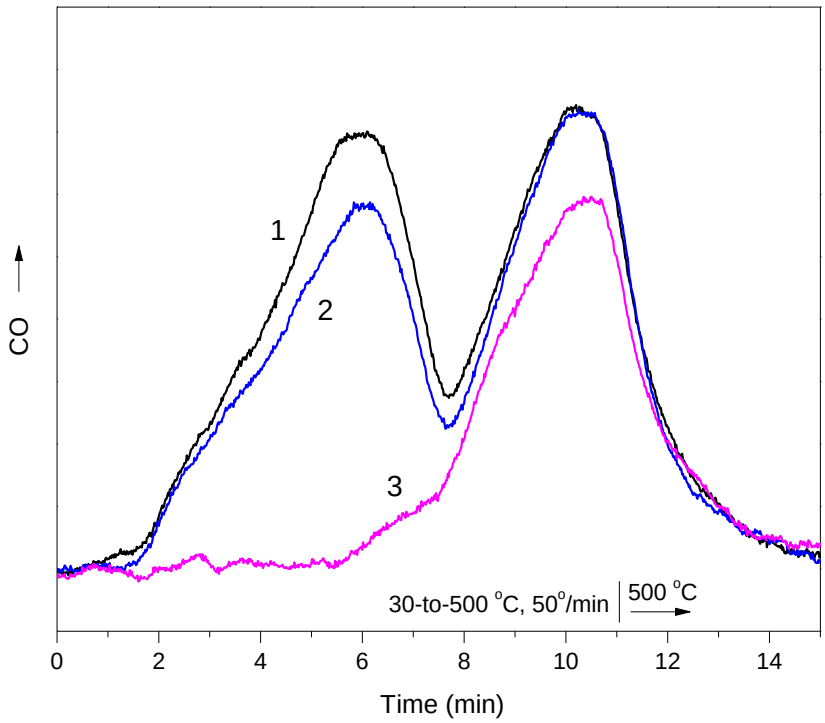

Fig. S3. Estimating the possible influence of O_2 impurities on CO-TPD pattern. In case 1, the 0.5%Pt/Al_2O_3 sample was pretreated under standard conditions (degassing, cooling, and CO pulsing, 20 min after degassing). In case 2, the exposure time in the flow of He at RT before CO dosing was increased to 2 h. In case 3, a pulse of O_2 was provided to the sample before CO pulsing (72 µl, O_{ads}/Pt = 0.46).

Both CO chemisorption and TPD run were performed with trapping CO_2 at 77 K, and the amounts of CO_2 accumulated in the trap in experiments 1-3 equaled to 2.4, 2.7, and 7.1 µmol, respectively. The additional quantity of CO_2 that was formed in experiment 3 (Δ_{3-1} 4.7 µmol) corresponds to the amount of O (4.6 µg-atom) that was intentionally pre-adsorbed, while the increment in CO_2 formation in run 2, Δ_{2-1}, is only 0.3 µmol.

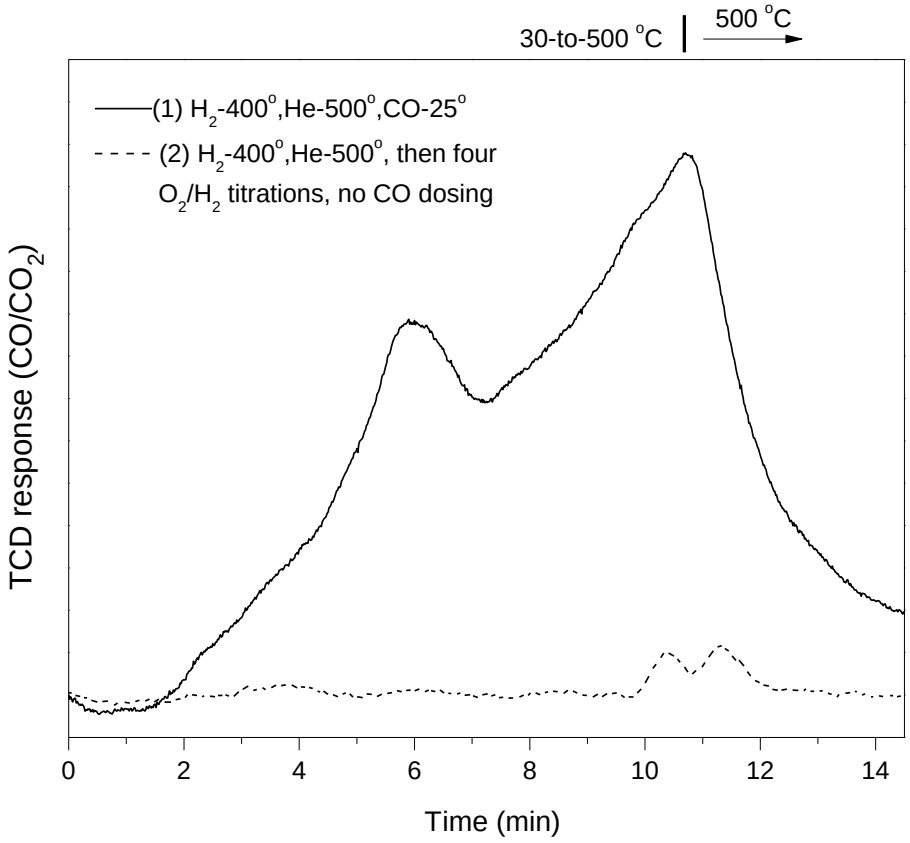

Fig. S4. Control experiments on the absence of carbonaceous species in the sample after its standard cleaning between successive runs. Here, solid curve shows CO/CO_2 desorption from a 0.5%Pt/γ-Al_2O_3 sample with preadsorbed CO; the trap before TCD was cooled to ~170 K to trap H_2O but to allow CO_2 to remain untrapped. Following the first run and cleaning procedures (section S2, protocol 2), TPD run was repeated without CO dosing; instead, four O_2/H_2 titrations were made, to facilitate desorption of carbon oxides if they are still present in the sample. The resulting (dashed) curve shows that some quantity of heavy gases evolves at high temperatures, but this quantity is negligibly small.

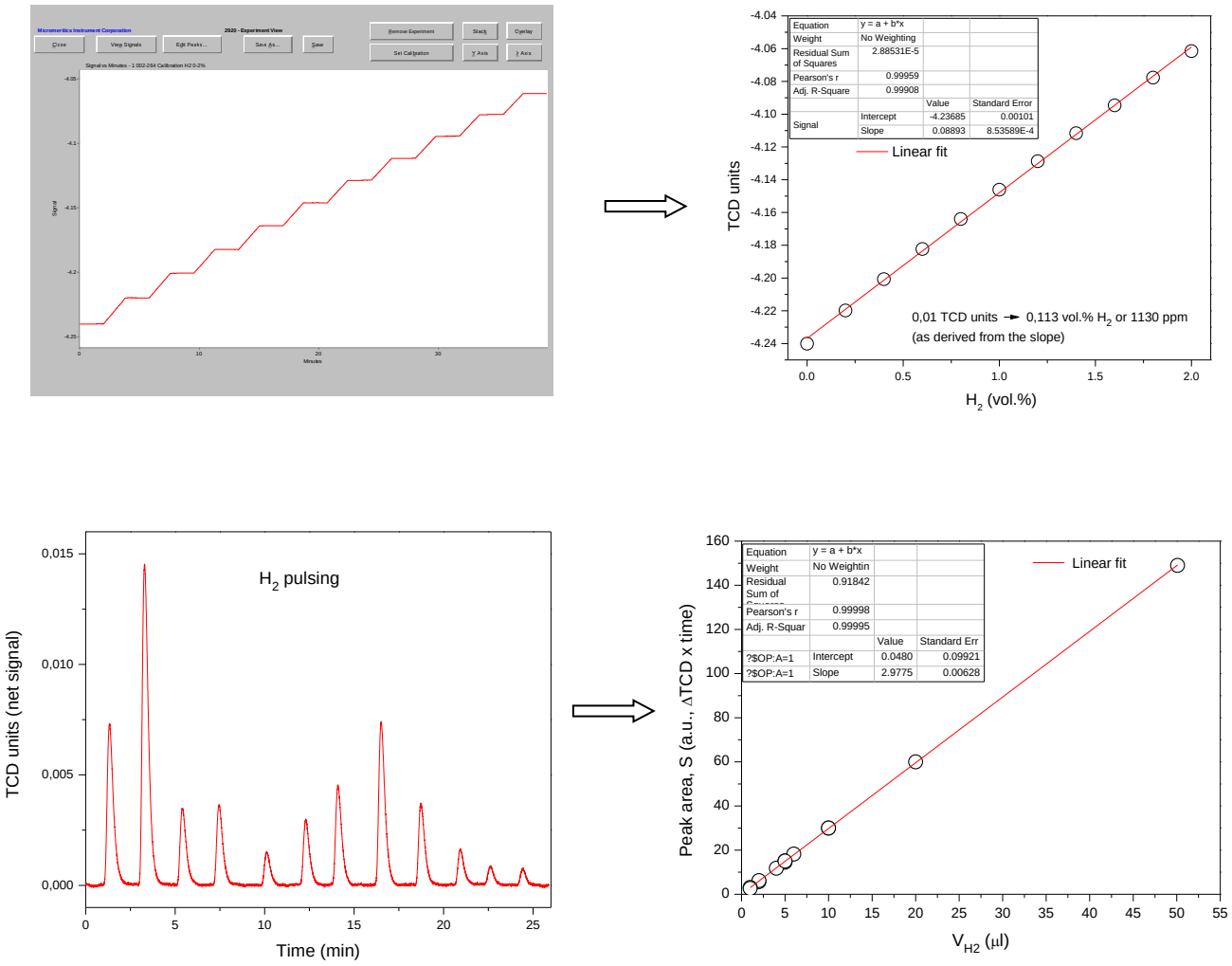

Fig. S5. Examples of calibration plots for H_2. The upper panel at right shows TCD signal vs. concentration of H_2, as found upon blending the flows of Ar and 2%H_2-in-Ar at varying ratios (shown at left). The two lower panels relate to the case when small amounts of H_2 were injected into the carrier gas by syringe; in the panel at right, X axis represents the amount of H_2 dosed, and Y axis shows the corresponding peak area.

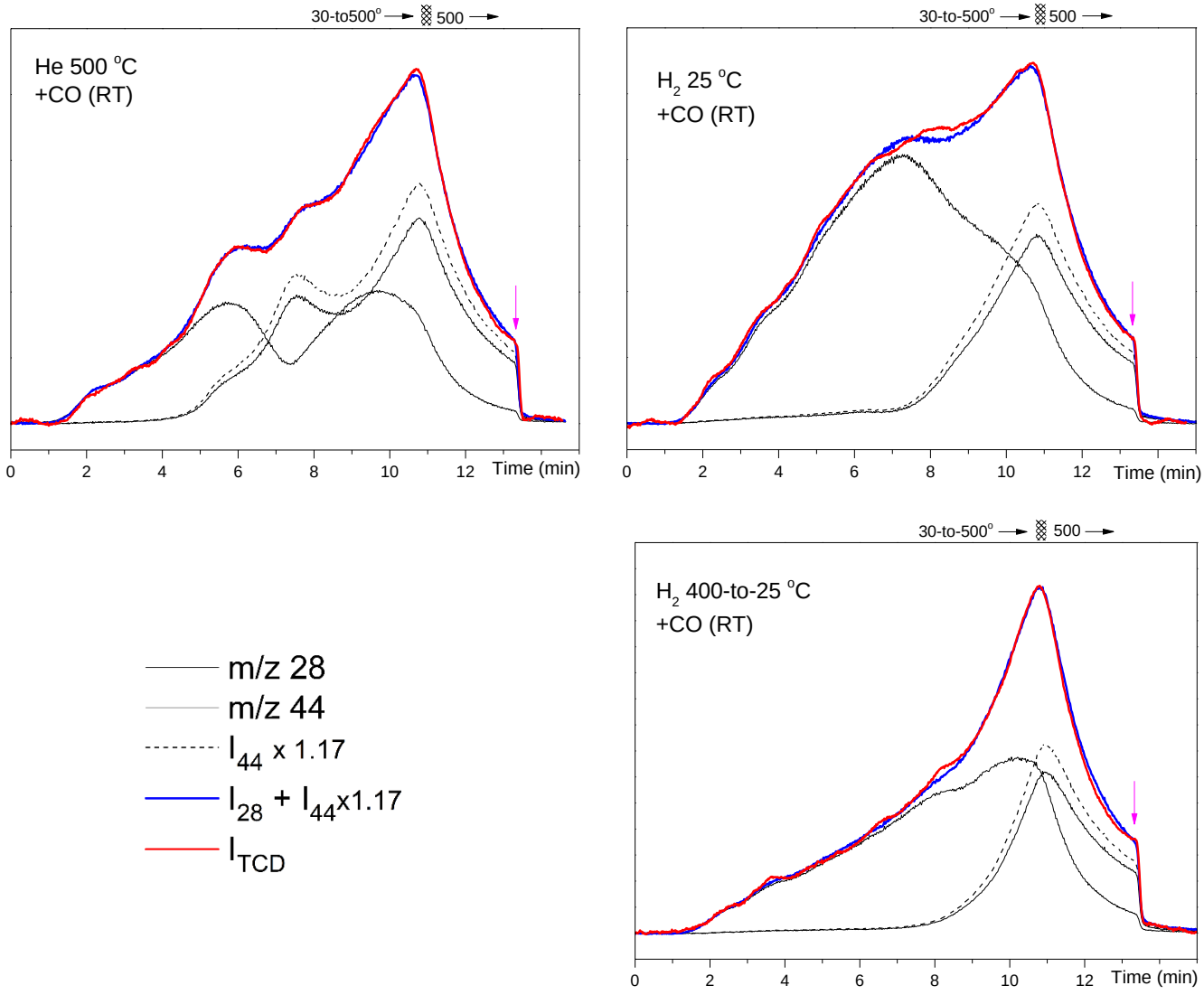

Fig. S6. Comparison of MS and TCD results for CO TPD from 0.5%Pt/γ-Al_2O_3 sample pretreated at different conditions (specified in the panels). Solid black curves represent molar concentrations of desorbing CO and CO_2 in the He carrier gas at a time *t*, as found with MS using corresponding calibrations and accounting for the CO_2-to-CO fragmentation. Blue curves show *an expected* response of TCD to the same gas mixtures; these curves were constructed by summation of the black curves (CO+CO_2) with account of the higher sensitivity of TCD to CO_2 (by a factor of 1.17, as shown in the Table in part S4). Real curves recorded with TCD in these experiments are shown by red lines, and one can see excellent agreement between the red and blue curves.

To provide an easy comparison, TCD intensities were arbitrarily normalized, and MS curves were slightly shifted to left, ~7 s, to compensate the longer time for the gas mixture to reach MS. Magenta arrows in the panels indicate the time when the carrier gas was directed to the detectors bypassing the sample, to check the baseline position.

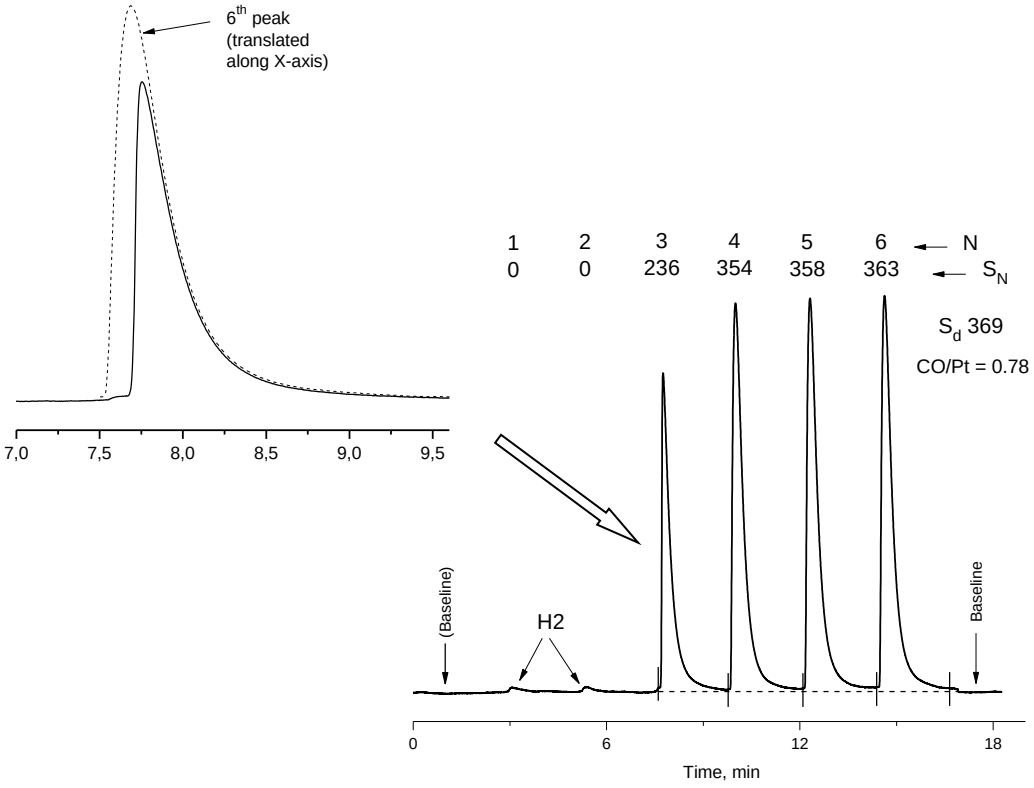

Fig. S7. Illustration of data treatment in CO pulse chemisorption measurements. The first two tiny peaks in the diagram relate to evolving H_2 and can be neglected, and the other peaks relate to unadsorbed CO. In the upper part of the figure (at left), the shape of the third peak is compared with that of the latest peak, and one can see that the first visible peak of CO looks like sharply truncated further peaks. This corresponds to the case of rapid adsorption. One can also see that the area of the sixth peak almost equals to that for the dose (S_d).

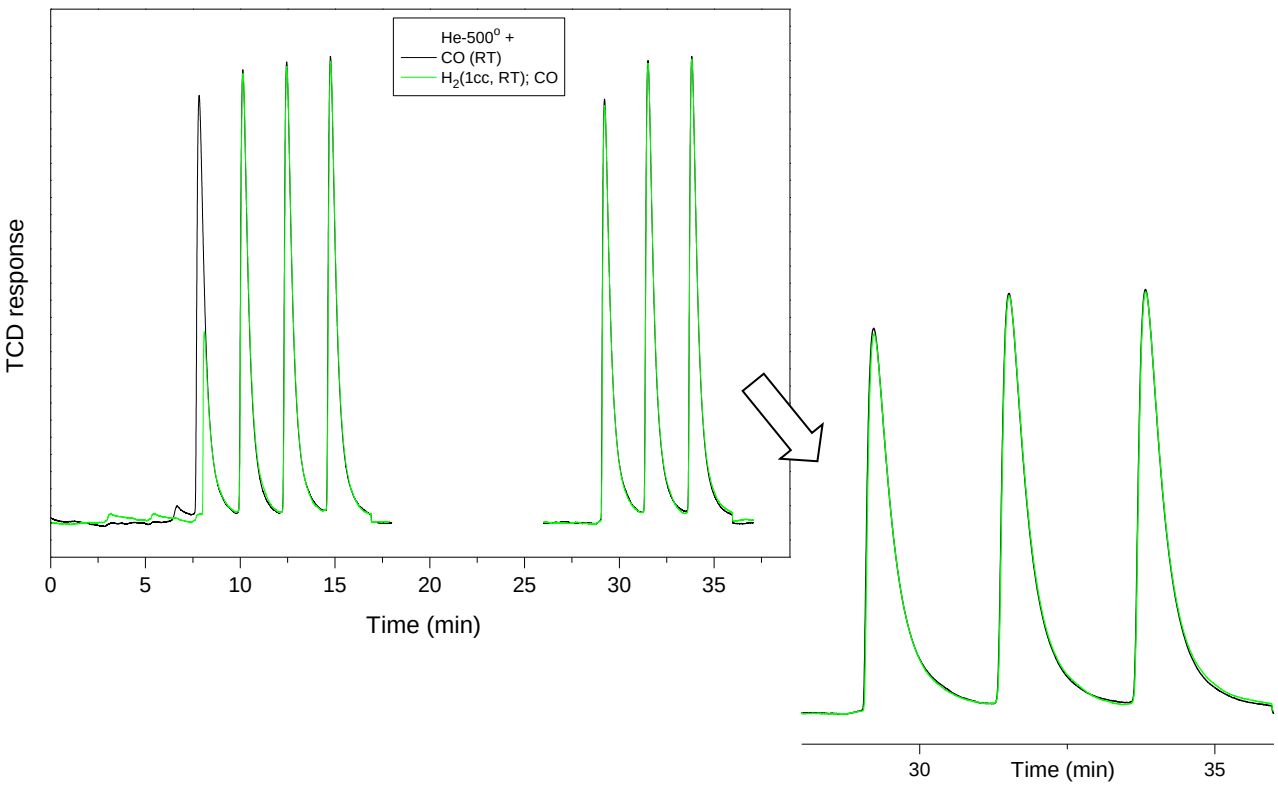

Fig. S8. Additional data for CO chemisorption on the preliminary degassed and on the H_2-covered 0.5%Pt/γ-Al_2O_3 (black and green curves, respectively; successive experiments with the same sample). Here, the samples were treated by six 72-μl doses of CO and were then left under He carrier gas for 10 min, after which time three new doses of CO were provided.

Considering the peaks after the additional doses, one can see that the first peak is slightly smaller than the latter ones. This is due to desorption of weakly bonded CO for the time of holding in the carrier gas (3-4 rel% to all CO adsorbed), so that a part of CO from the new dose can be absorbed to replenish CO coverage. At the same time, the black and greed peaks in this region practically coincide, thus indicating that both the samples behave similarly and the first six doses of CO were enough to saturate the samples.

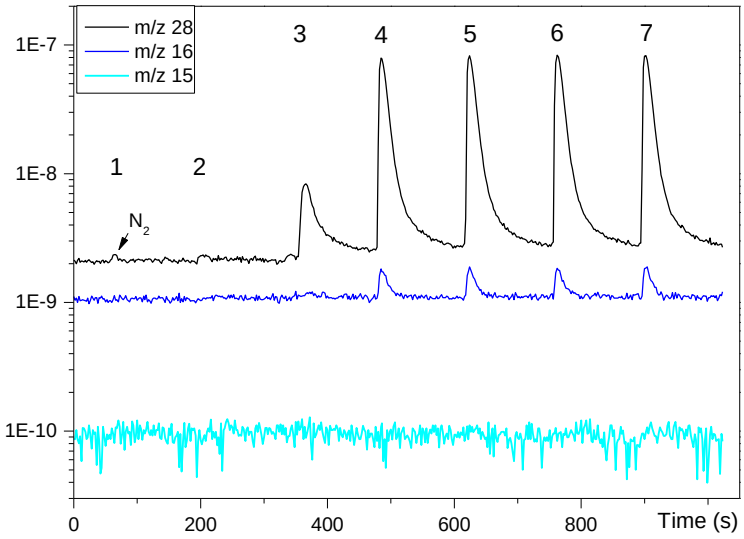

Fig. S9. MS data for CO pulse chemisorption on H_2-pretreated 0.5%Pt/γ-Al_2O_3.

The barely perceptible peaks at m/z 28 from the first two injections of CO relate to N_2 impurity in CO (note that Y axis in this panel is plotted on logarithmic scale and the content of N_2 is negligibly small as compared to CO). The signals at m/z 16 results from CO fragmentation, but there are no visible m/z 16 signals after the first two doses of CO (which were completely consumed by the sample). Neither there are visible m/z 15 signals, which would signal for the formation of methane. (In mass spectrum of methane, the signals from CH_4^+ and its CH_3^+ fragment have similar intensities.)

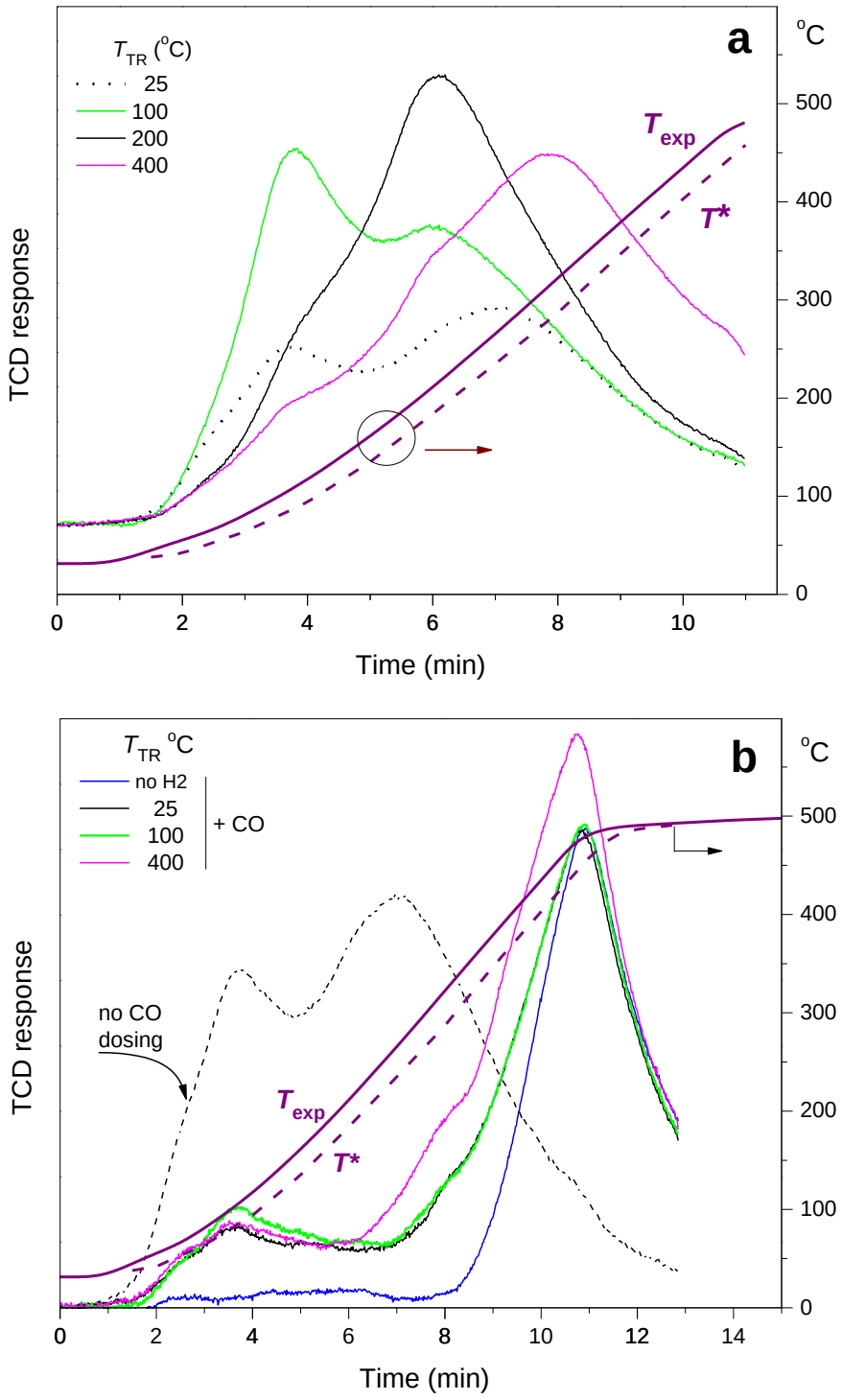

Fig. S10. Temperature-*vs*-time plots (purple lines) corresponding to TPD conditions in Fig. 4 in the main text (a) and in Fig. S15 (b). T_{exp} is the sample temperature at a time *t*, and *T** corresponds to the time of detector response (see explanation in section S4).

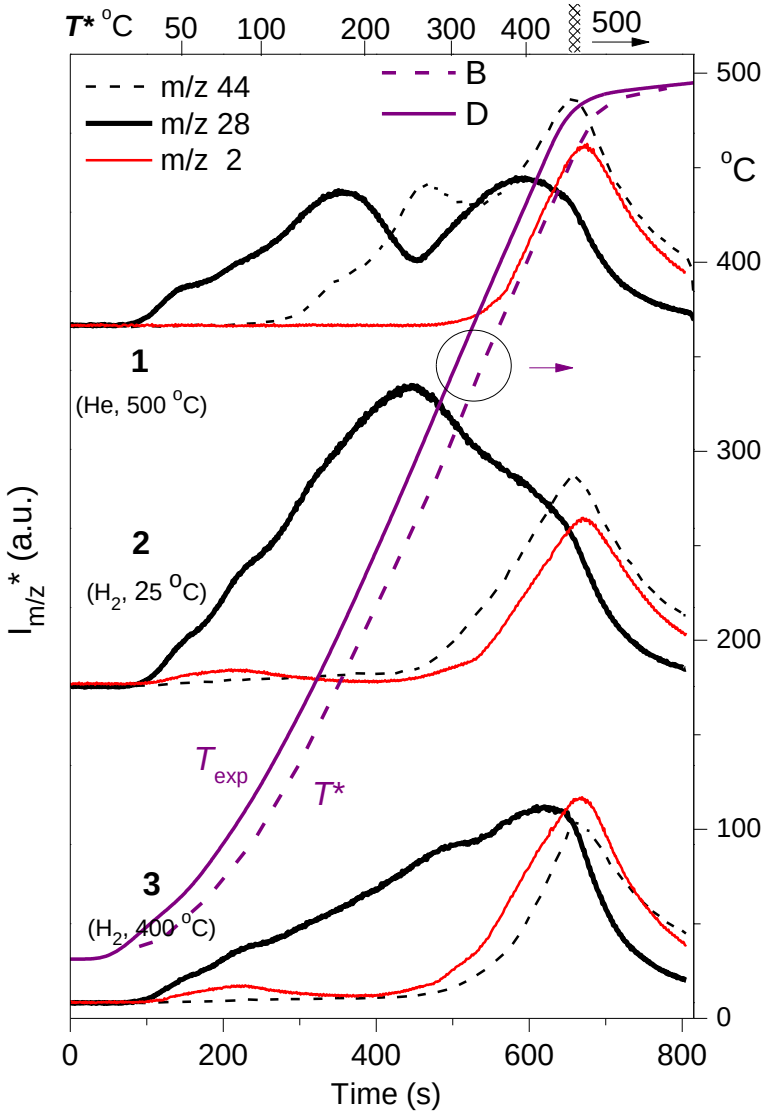

Fig. S11. Temperature-*vs*-time plots (purple lines) corresponding to TPD conditions in Fig. 5 in the main text. T_{exp} is the sample temperature at a time *t*, and *T** corresponds to the time of detector response (see explanation in section S4).

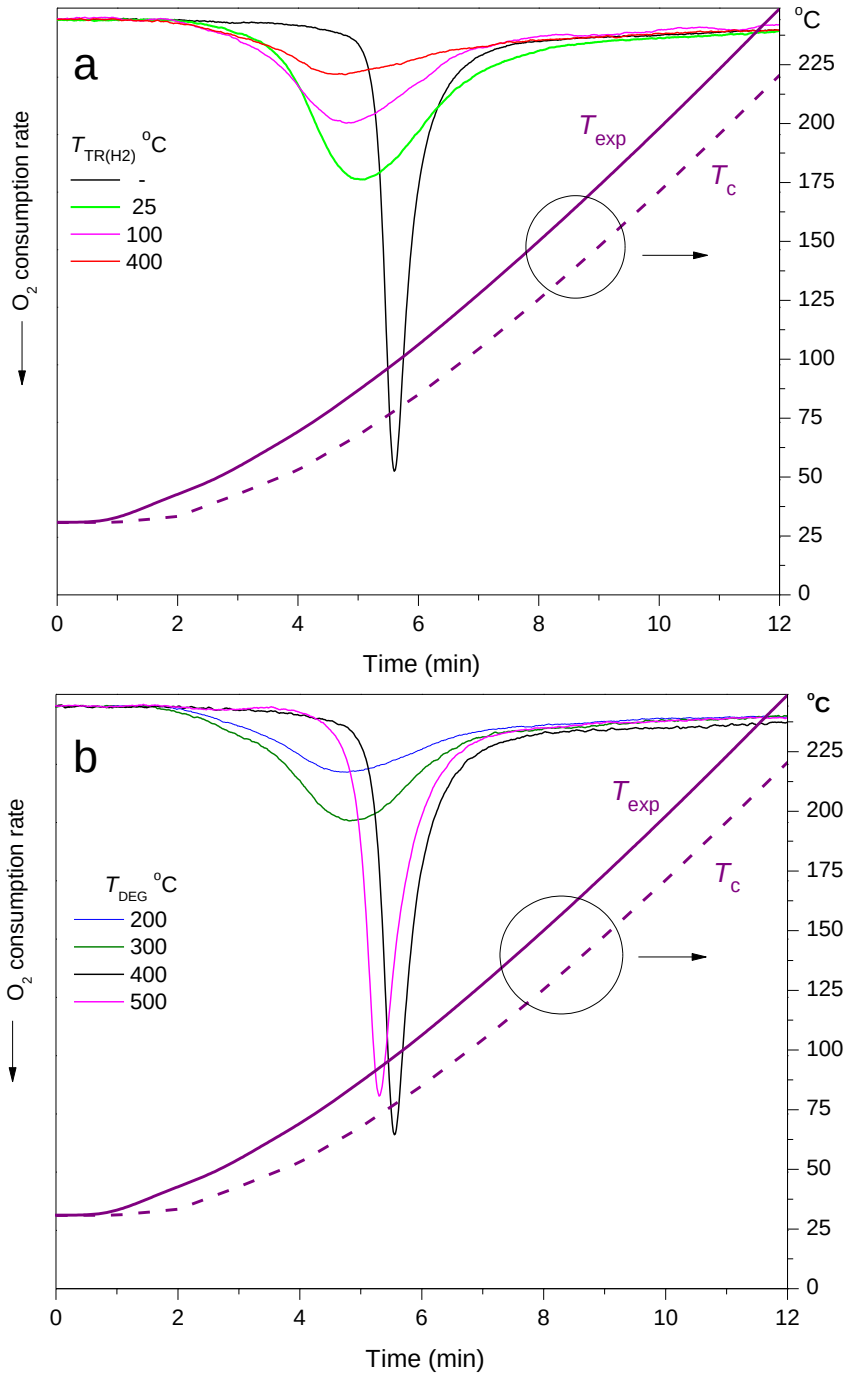

Fig. S12. Temperature-vs-time plots (purple lines) corresponding to TPO conditions in Fig. 7 in the main text.

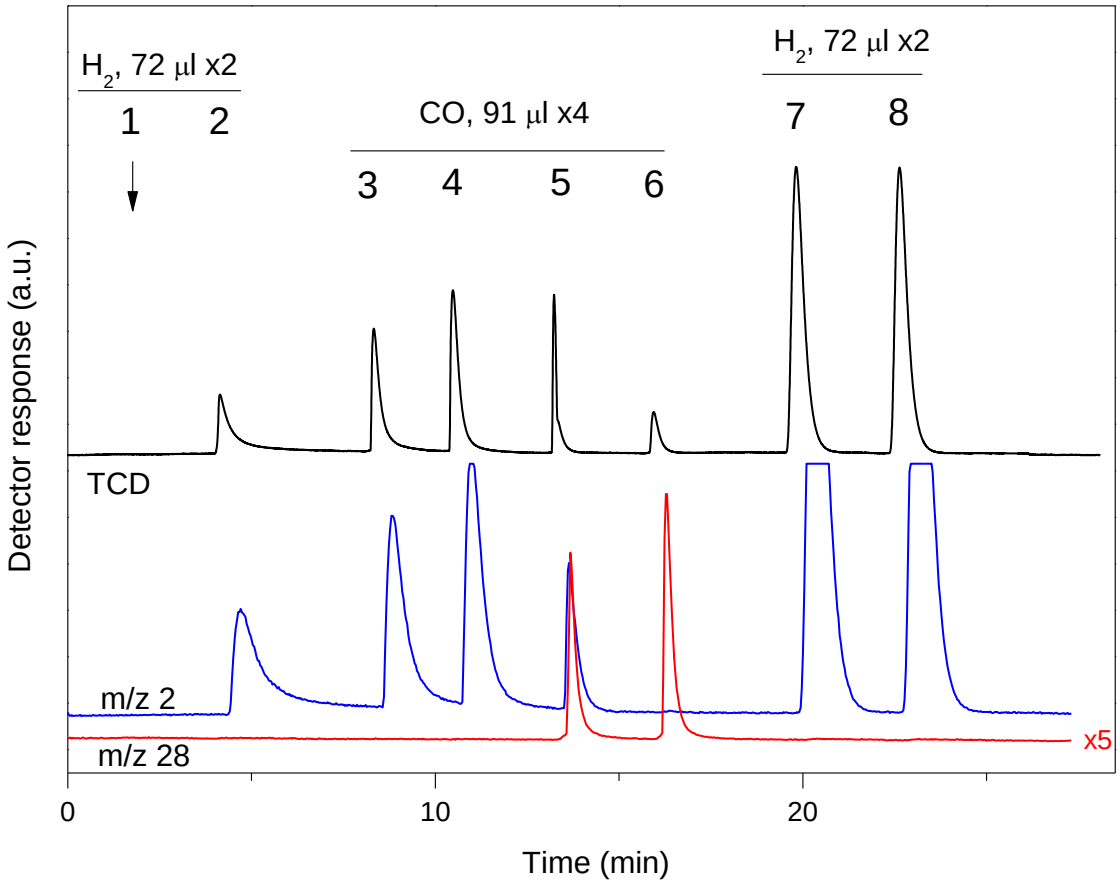

Fig. S13. An experiment on H_2-by-CO displacement, with simultaneous monitoring of the process by TCD and MS. Here, Ar was used as the carrier gas, and the preliminary degassed 0.5%Pt/γ-Al_2O_3 sample was consecutively treated by two doses of H_2, four doses of CO, and (again) two doses of H_2. The MS data show that there are only H_2 in the effluent gas after the first two doses of CO, and only CO (without H_2) after the forth dose of CO; moreover, MS detects no CO in the carrier gas after additional injections of H_2. As measured with TCD (see Tables on the next page), the areas of peaks 7 and 8 (black curve) are equal and correspond to the dosing amount of H_2. It follows that H_2 does not further adsorb on the (H_2+CO) treated sample and does not displace the adsorbed CO, at least, in appreciable amounts.

Peak areas (TCD, a.u.), as found in the experiment in Fig. S13 (experiment 1) and in repeated experiment (2) when the sample was kept under the Ar carrier gas for a longer time. Total time in Ar before hydrogen chemisorption: 20 min (1) and 50 min (2).

No.	Injections	*S* (a.u.)	
		Experiment 1	Experiment 2
1	H_2, 72 µl	0 (H_2 unadsorbed)	0 (H_2 unadsorbed)
2	H_2, 72 µl	69 (H_2 unadsorbed)	59 (H_2 unadsorbed)
3	CO, 91 µl	81 (H_2 displaced)	83 (H_2 displaced)
4	CO, 91 µl	99 (H_2 displaced)	93 (H_2 displaced)
5	CO, 91 µl	46 ($\Sigma H_{2,displaced}$+$CO_{unadsorbed}$)	44 ($\Sigma H_{2,displaced}$+$CO_{unadsorbed}$)
		26, for H_2 displaced*	24, for H_2 displaced*
6	CO, 91 µl	23.5 (CO)	24.3 (CO)
7	H_2, 72 µl**	245	244
8	H_2, 72 µl**	245	243

*As found with account of the S_5/S_6 ratio for m/z 28.

**S_0 value for such a dose corresponds to 244±1 units, as found using an empty tube, before and after these experiments.

From the data in the Table above and with account of sample mass (here, 408 mg) we have:

	Experiment 1	Experiment 2
$H_{adsorbed}/Pt$* (atomic ratio)	1.04	1.06
$H_{CO\text{-}displaced}/Pt$ (atomic ratio)	0.512	0.495
CO_{ads}/Pt	0.893	0.894

The difference between the results of these two experiments can be considered negligible, thus confirming that the content of O_2 impurities in the carrier gas is too small to affect the results.

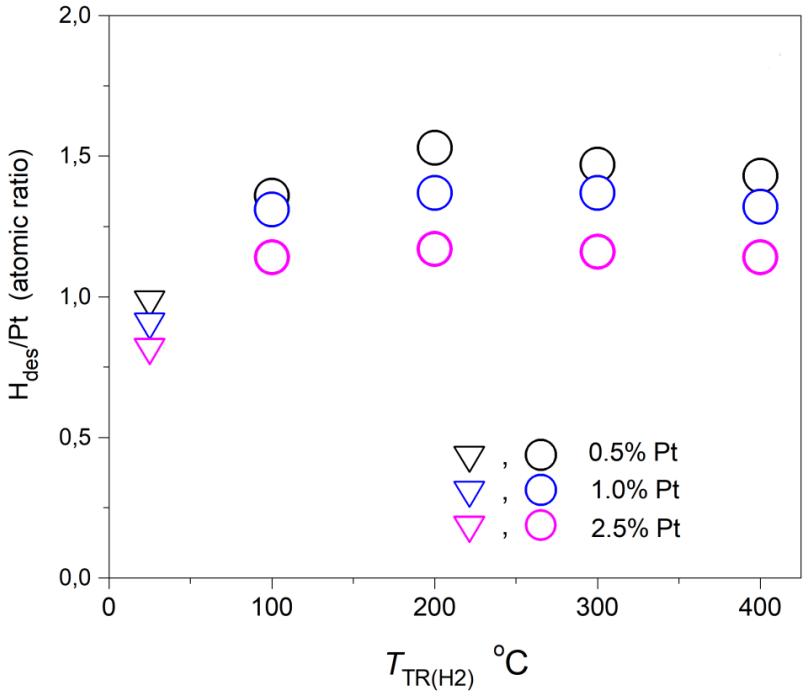

Fig. S14. The amounts of H_2 desorbed in TPD runs from Pt/γ-Al_2O_3 samples with different Pt loading, in dependence on H_2-pretreatment temperature (H_2 pulsing at 25 °C and flowing H_2 in the other cases). The H_{des}/Pt values were calculated from the data in ref. S2 and include hydrogen that was evolved during sample heating to 500 °C plus isothermal hold for 3 min at final temperature.

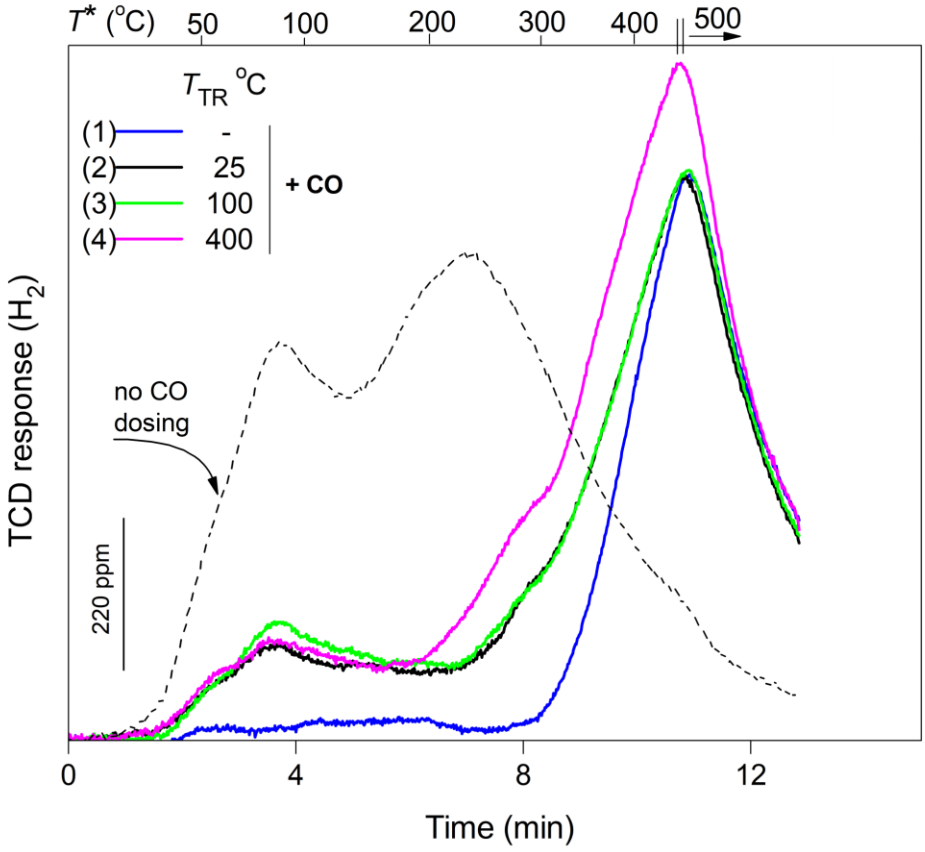

Fig. S15. TCD data for H_2 TPD from 0.5%Pt/γ-Al_2O_3 after room-temperature CO chemisorption on preliminarily degassed sample (1) and on H_2-pretreated sample (2-4). For comparison, the dashed curve from Fig. 4, corresponding to $T_{TR(H2)}$ of 25 ºC without further CO treatment, is also provided. Ar was used as the carrier gas, and the weak signals at the low and moderate temperatures in case 1 (blue curve) relate exclusively to heavy gases, CO/CO_2 (as checked with MS).

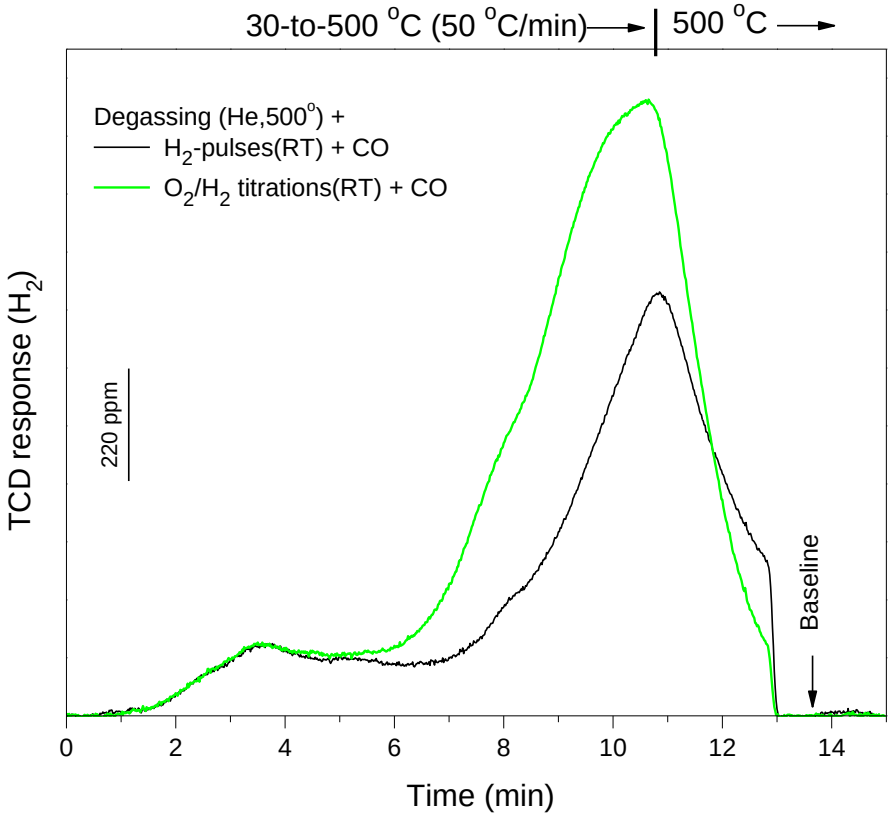

Fig. S16. H_2 TPD runs under standard conditions (black curve) and in the presence of a small amount of H_2O generated through O_2/H_2 titrations (green curve). In the latter case, the 0.5%Pt/γ-Al_2O_3 sample was degassed and then treated at room temperature in the following order: H_2→He→O_2(pulses)→H_2(5min)→He(7 min)→CO(pulses).

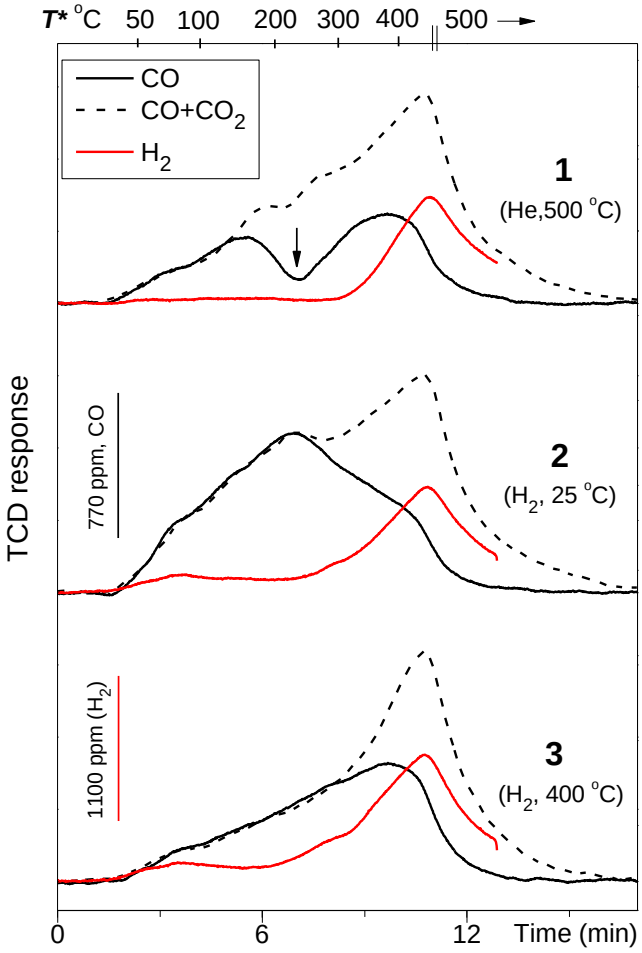

Fig. S17. Experiments as in Fig. 5 in the main text but using TCD. Ar as the carrier gas for detecting H_2 and He for CO and CO_2. The black dashed curves were recorded with trapping only H_2O (170 K), and the detector reacted both to CO and CO_2. The black solid curves were recorded with trapping CO_2 at 77 K; to compensate the longer retention time in this case (for the gas mixture on the way to detector), the original CO-TPD curves were slightly shifted along X-axis to left, by 0.7 min. The Table below lists the amounts of CO_2 accumulated in the trap, along with CO adsorption/desorption data for these runs.

Treatment before CO adsorption	CO_{ads}/Pt	CO_{ads} µmol	CO_{des} µmol	$CO_{2,des}$ µmol	$CO_{des}+CO_{2,des}$ µmol
He, 500 °C	0.66	**7.0**	3.1	3.1	**6.2**
H_2, 25 °C	0.85	**8.9**	5.7	2.4	**8.1**
H_2, 400 °C	0.61	**6.4**	4.2	1.9	**6.1**

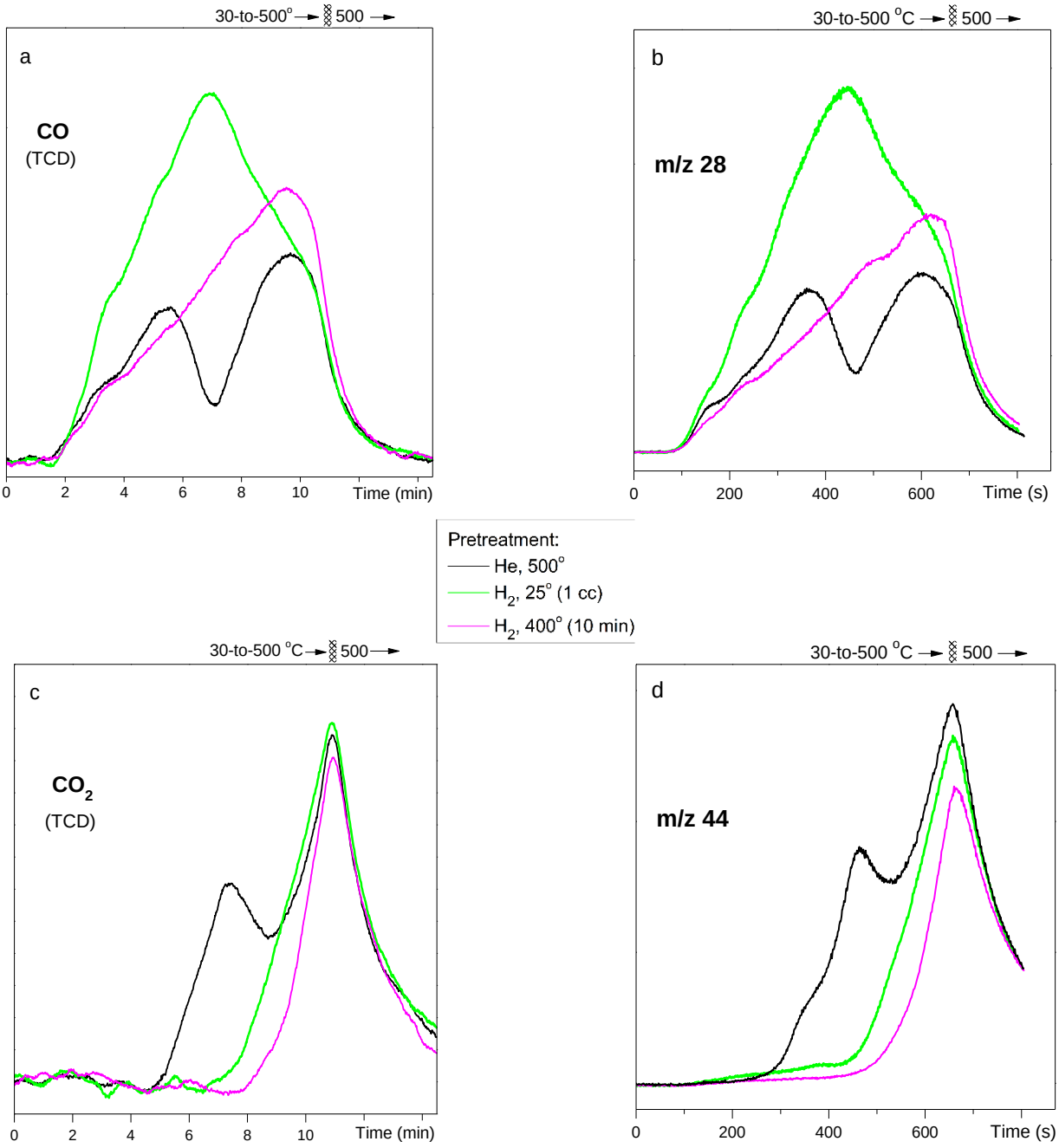

Fig. S18. CO/CO_2 curves from Fig. S17 (a, c) and from Fig. 5 in the main text (b, d), as grouped accordingly to desorbing gas. The curves in (c) represent difference curves that were obtained by subtraction of solid black curves in Fig. S17 from corresponding dashed black curves.

The experiments with TCD and mass-spectrometry detections were performed at different times, and the difference between the curves at left and right is mainly due to this factor.

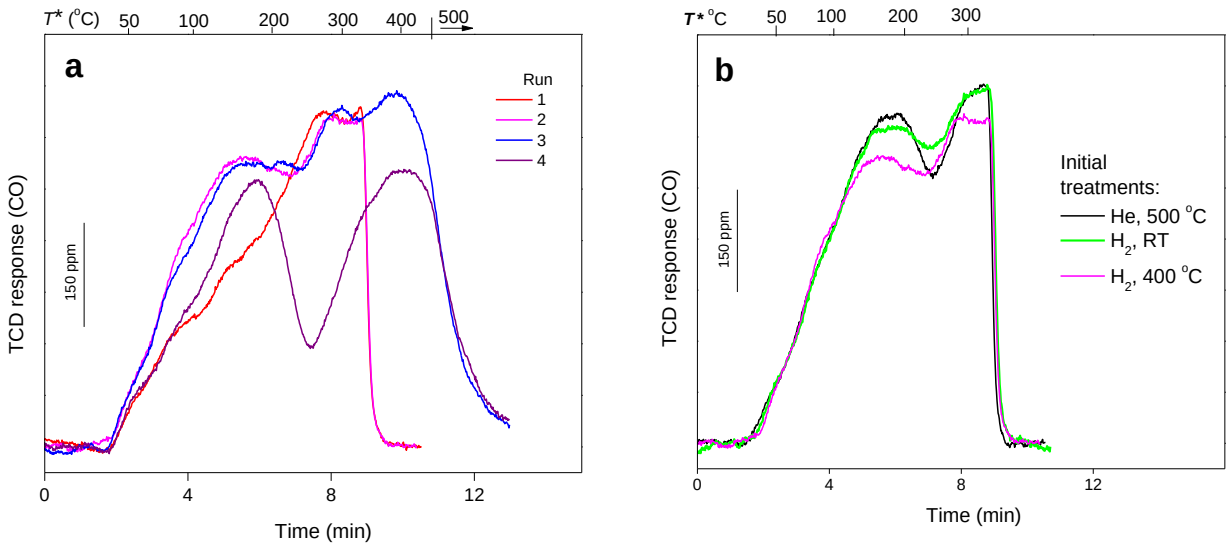

Fig. S19. Supplementary data to Fig. 6b in the main text.
(a) Successive CO-TPD runs with the sample that was initially treated under H_2 at $T_{TR(H2)}$ of 400 ºC. Run 3 was conducted with heating the sample up to 500 ºC, and run 4 was performed after annealing the sample at that temperature (after run 3, the sample was kept under the carrier gas at 500 ºC for 15 min).
(b) CO-TPD traces recorded in the *second* runs for the samples that differ in conditions of initial treatments.

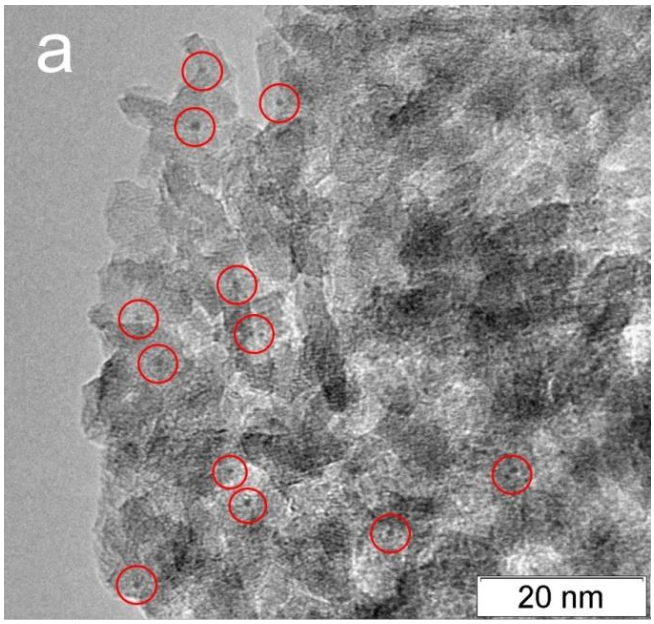

Fig. S20. Characteristic TEM image of 0.5%Pt/γ-Al_2O_3 after 18 TPO runs, including the two series of experiments in Fig. 7 in the main text. For clarity, some of the Pt clusters are marked by red circles.

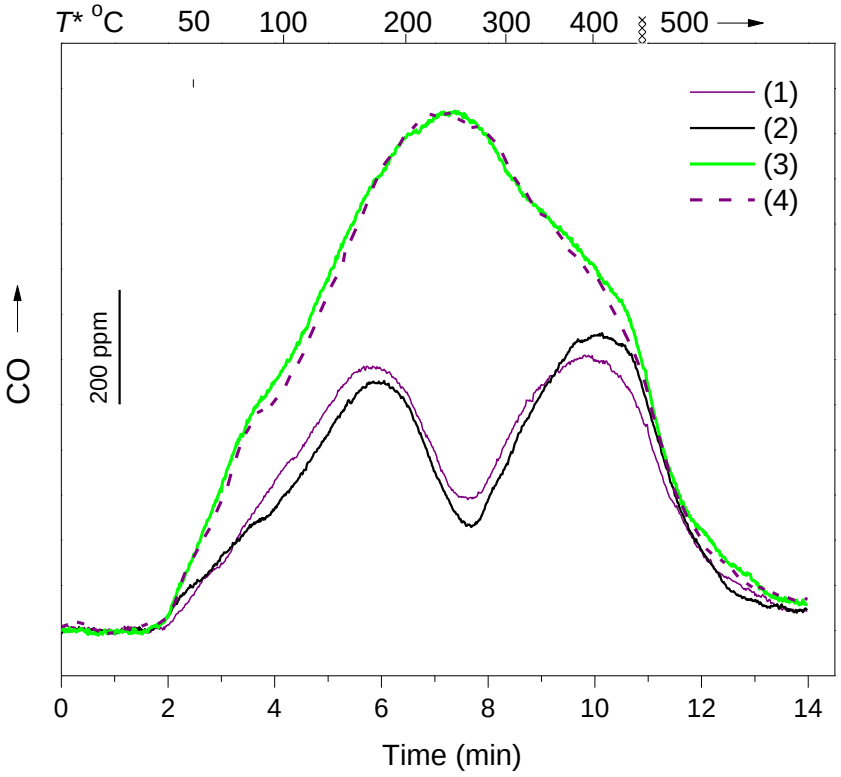

Fig. S21. Supplementary data to Fig. 8 in the main text. Purple curves (1 and 4) are the same as curves 1 and 4 in Fig. 8; here they are compared with CO-TPD curves for H_2-*un*treated sample (2) and for the sample that was treated with H_2 *before* CO dosing (3).

Sequence and conditions of treatments after sample degassing:
(1) CO (six 72-µl doses); H_2 (1-cc pulse, 15 s after the last CO pulse).
(2) CO (six 72-µl doses).
(3) H_2 (a flow, 5 min); CO (six 72-µl doses, 5 min after H_2 treatment).
(4) CO (six 72-µl doses); H_2 (a flow, 5 min); CO (three 72-µl doses, 5 min after H_2 treatment).

All pretreatments at room temperature.

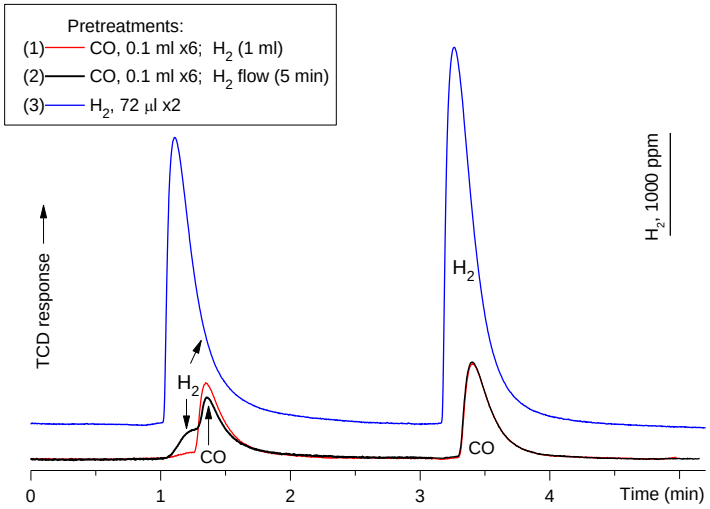

Fig. S22. H_2 displacement by 0.1-ml pulses of CO from 0.5%Pt/γ-Al_2O_3 sample. The upper (blue) curve relates to sample that was degassed and then treated only with H_2, and the two lower curves correspond to the case when H_2 treatment was given to CO-covered sample. Five minutes intervals were inserted between the CO-H_2-CO treatments. The data show that only a long treatment of CO-covered sample in flowing H_2 affords an appreciable (but very small) quantity of H_2 that can be further displaced by CO.

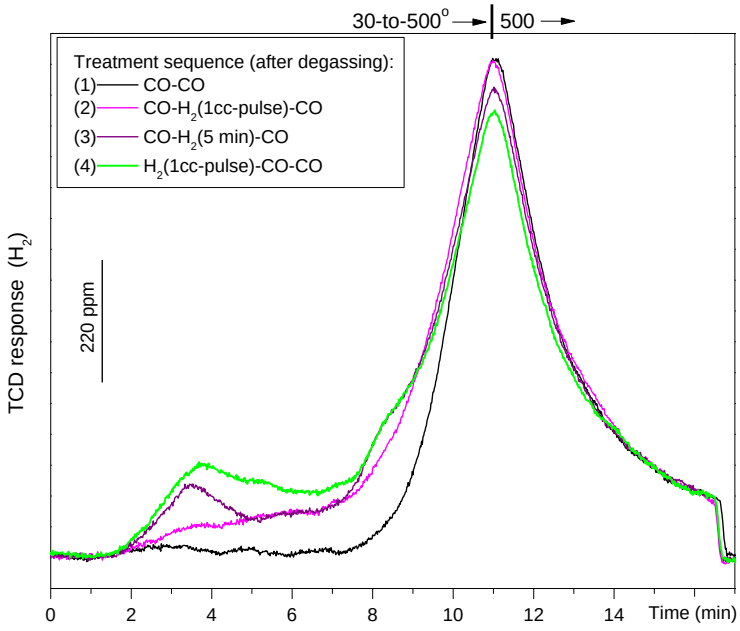

Fig. S23. H_2-TPD curves of 0.5%Pt/γ-Al_2O_3 sample after treating it with H_2 and CO in different order. Here, CO was dosed in two steps: first, six 72-µl pulses of CO were made, and 10 min later three new doses were delivered. Hydrogen was provided before CO dosing (case 4) or between the first and last CO doses (curves 2 and 3). In case 1, H_2 treatment was omitted.

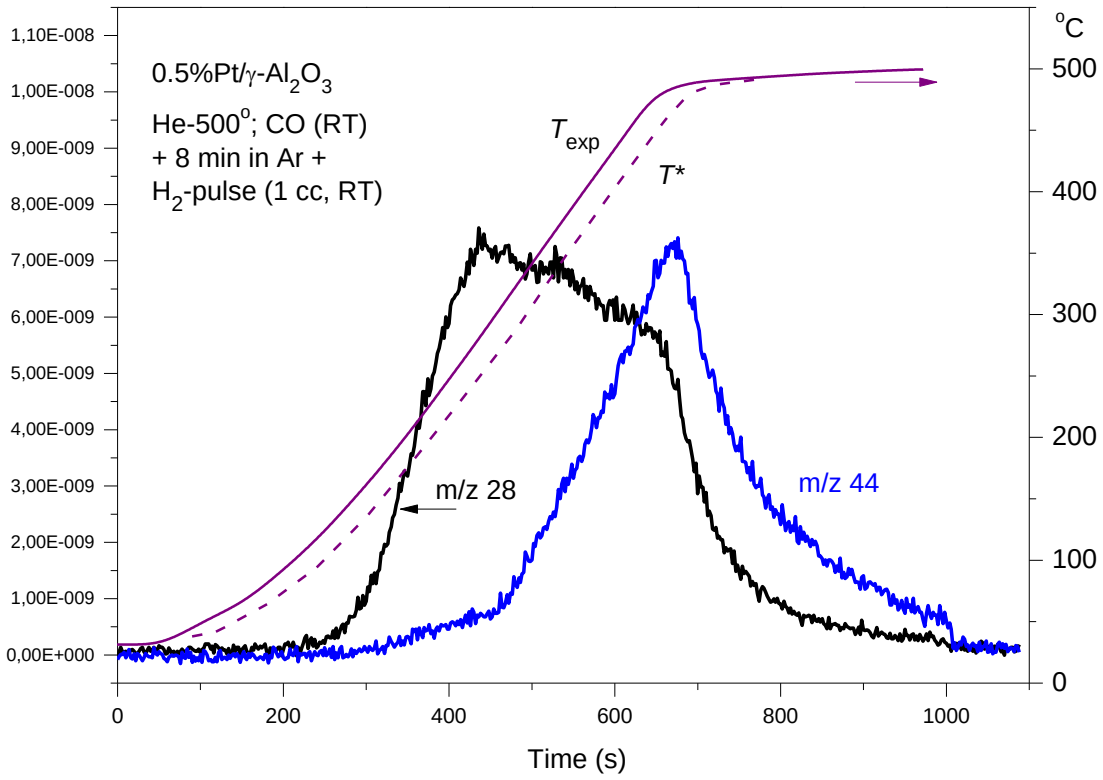

Fig. S24. MS data relevant to Fig. 8 in the main text. Here, the CO-covered sample was left under the carrier gas for 8 min, and 1-cc pulse of H_2 was then provided. Black curve shows CO TPD trace and blue curve shows CO_2 trace (the trap was at 170 K).

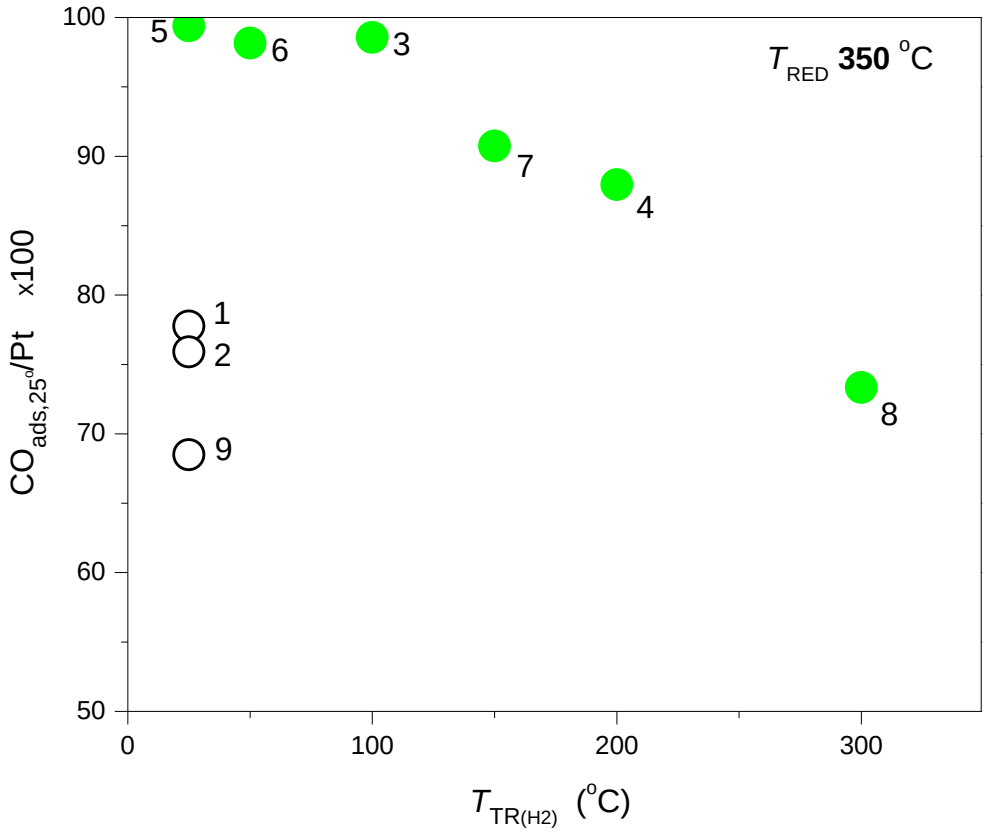

Fig. S25. CO pulse chemisorption data for 0.5%Pt/γ-Al_2O_3 sample that was initially reduced at 350 °C (90 min). Following these experiments, the sample was treated in flowing H_2 at 500 °C for 30 min, and a new series of experiments, presented in Fig. 1b in the main text, was performed.

The trends in this figure are similar to those in Fig. 1b, but one can notice that the freshly reduced sample in Fig. S25 demonstrates somewhat lower stability during successive runs as compared to the stabilized sample in Fig. 1b.

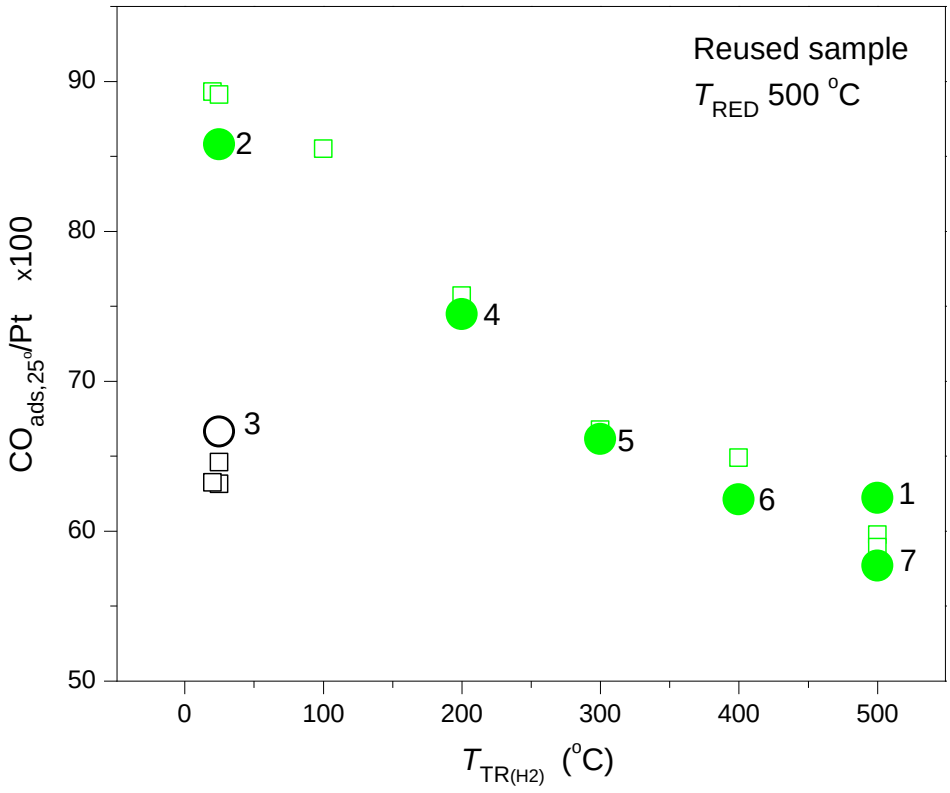

Fig. S26. Repeated testing of 0.5%Pt/γ-Al_2O_3 sample. After the experiments in Fig. 1b in the main text, the sample tube was disconnected from the instrument and the sample was stored for about a year. It was then reoxidized at 500 ºC and rereduced at 500 ºC. The data from Fig. 1b are also provided for comparison (small squares).

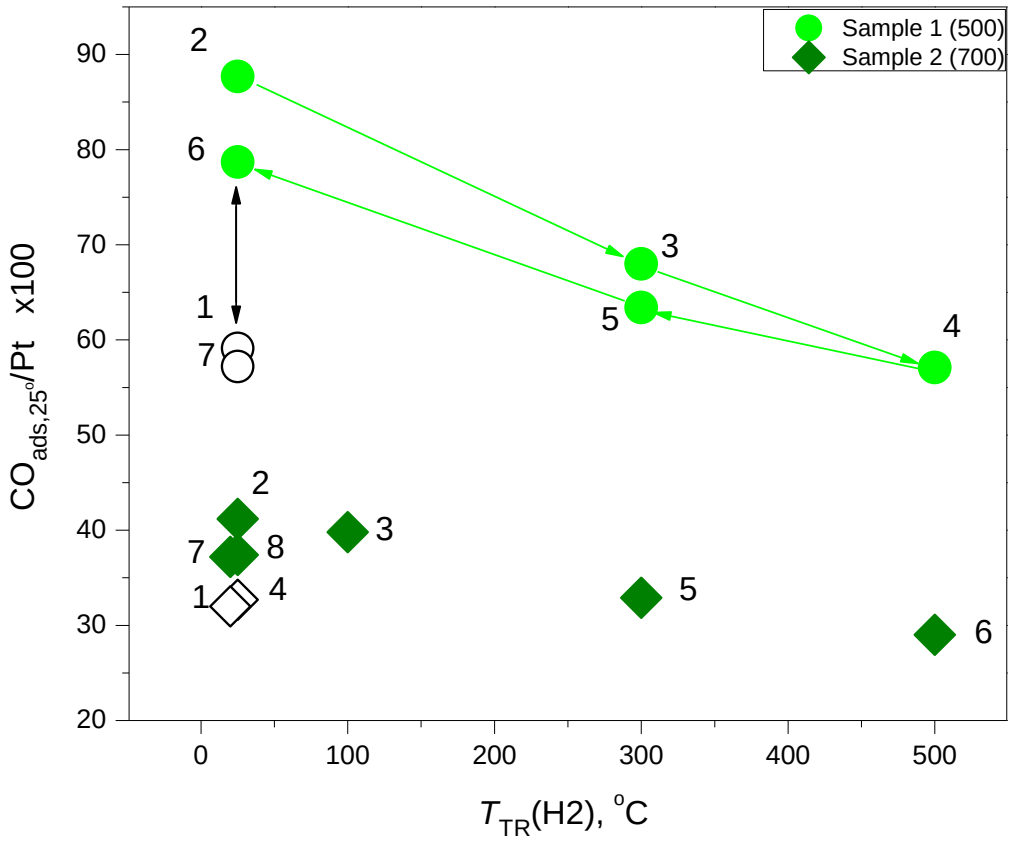

Fig. S27. Comparative experiments with a 0.43%Pt/γ-Al_2O_3 catalyst representing Russian analog of EUROPt-3 standard catalyst (courteously granted by Dr V.B. Goncharov from our Institute). The catalyst was produced in extruded form and was earlier reduced in small quantities at 500 and 700 °C (sample 1 and 2, respectively). Before these experiments, the extrudates were gently crushed in a mortar, and the resulting samples (by 400 mg each) were reoxidized (O_2, 300 °C, 30 min) and rereduced (H_2, 300 °C, 30 min) in situ. The numbers near the symbols show the sequence order of the measurements; open symbols refer to degassed samples.

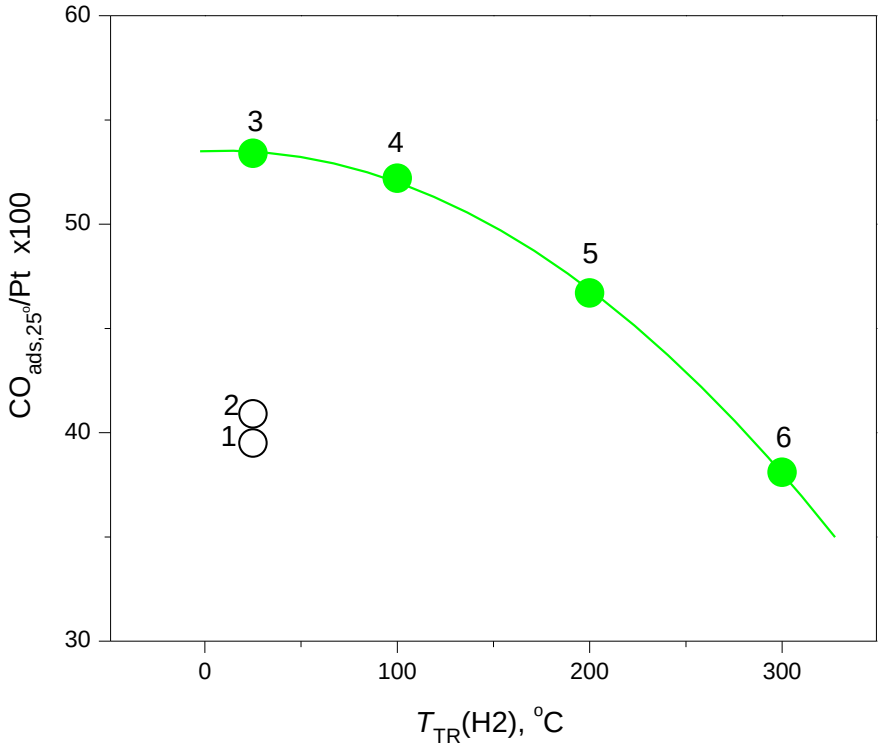

Fig. S28. Comparative experiments with a Cl-free 0.6%Pt/γ-Al_2O_3 catalyst (courteously provided by Dr E.V. Kovalev from our Institute). The sample was prepared with the use of Pt acetylacetonate and home-made support and was previously used in experiments on CO oxidation. Before the chemisorption measurements, the sample was re-oxidized (O_2, 300 °C, 30 min) and re-reduced (H_2, 300 °C, 30 min) in situ. The numbers near the symbols show the sequence order of the measurements; black open symbols refer to degassed sample.

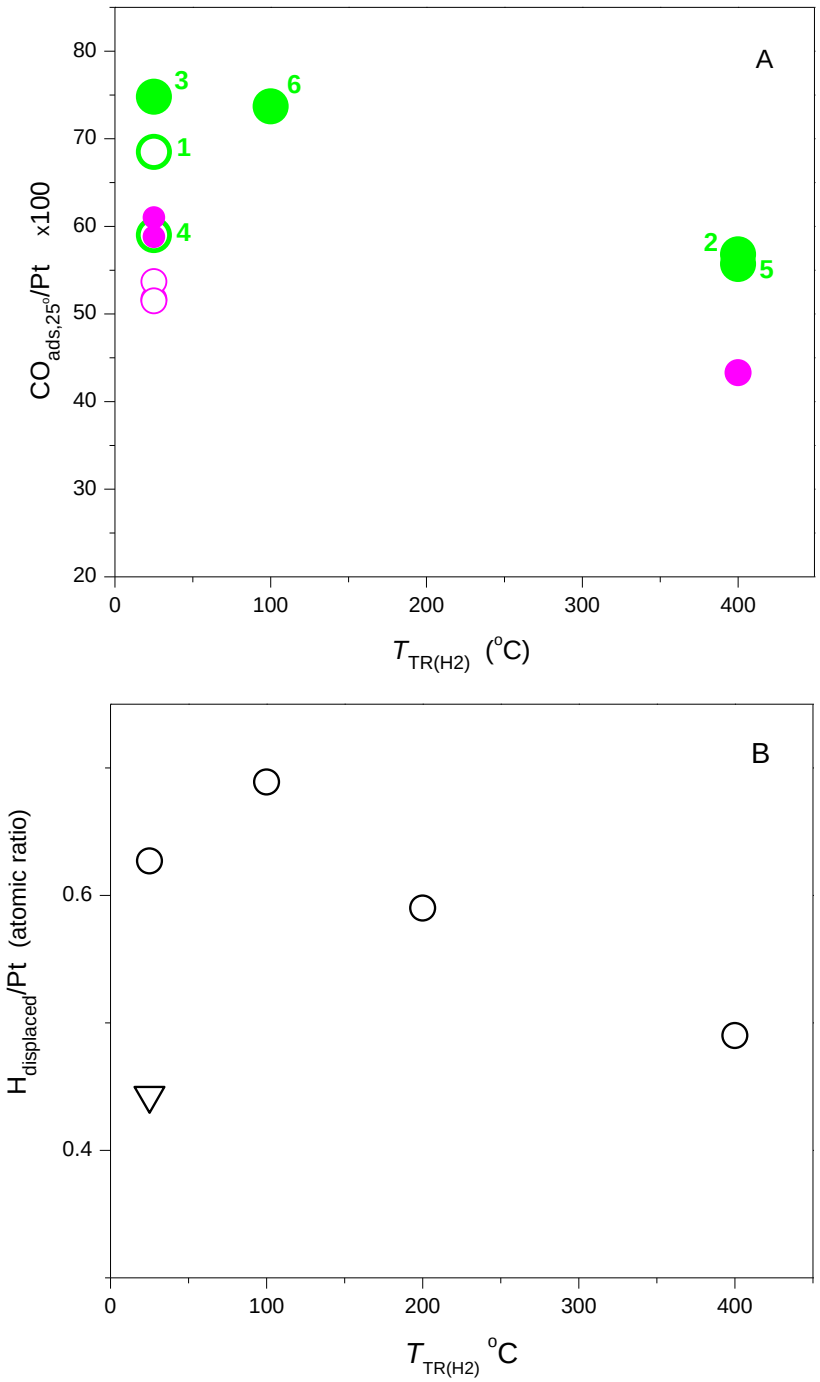

Fig. S29. CO pulse chemisorption (A) and H_2-by-CO displacement data (B) for Pt/γ-Al_2O_3 sample with a high Pt loading (2.5 wt%). In panel A, green symbols shows a series started with freshly reduced sample, and magenta symbols refer to aged sample (after two different series, with storage, reoxidation, and rereduction). In panel B, triangle stands for pretreatment by H_2 pulses and circles for pretreatments in a flow of H_2.

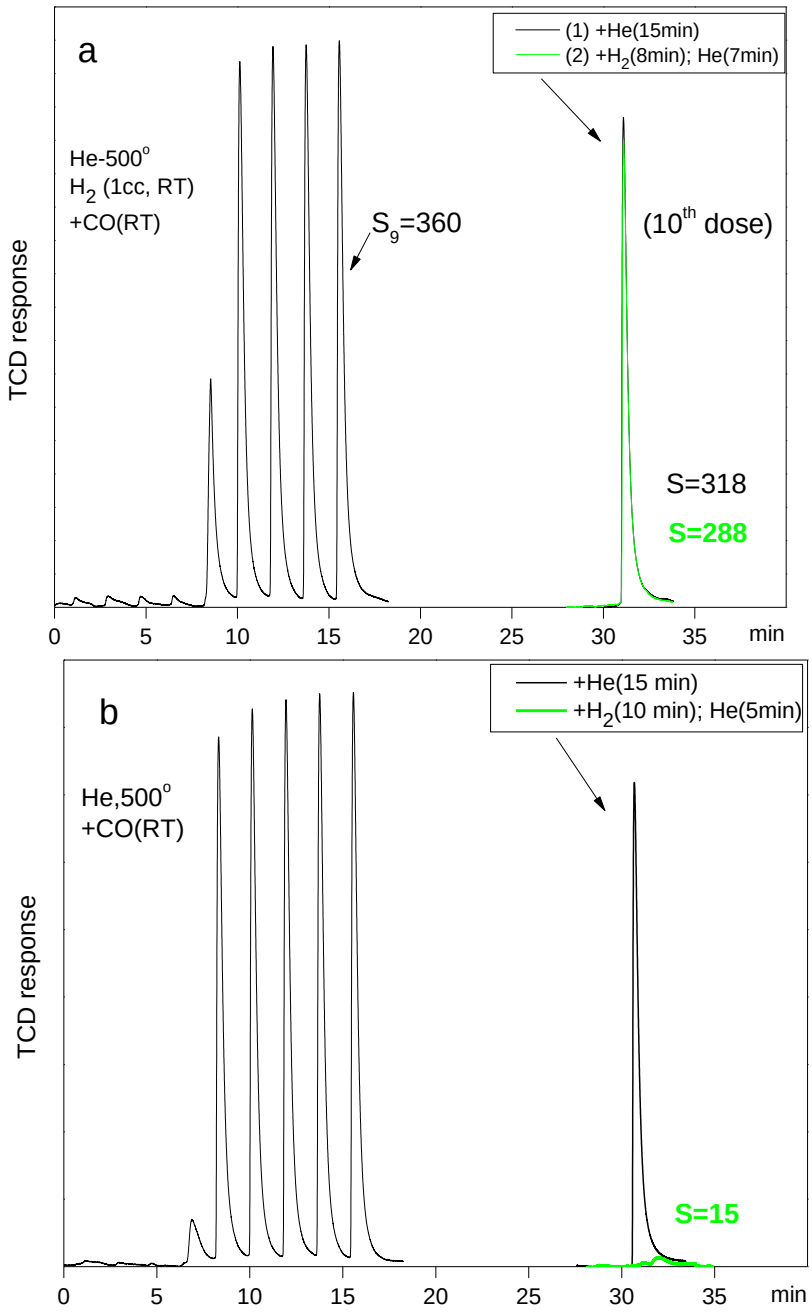

Fig. S30. CO chemisorption results for 2.5%Pt/γ-Al_2O_3 sample (200 mg), which was preliminary treated with H_2 (a) or used directly after degassing (b). Following the injection of nine 72-μl doses of CO, the sample was left for 15 min under the He carrier gas or under a flow of H_2, and a new dose of CO was then provided. S values near the 10^{th} peak show peak areas (a.u.). One can notice that the sample in (a) adsorbs small amounts of CO from the 10^{th} dose, but the intermediate H_2 treatment in case (b) results in almost complete consumption of the 10^{th} CO dose.

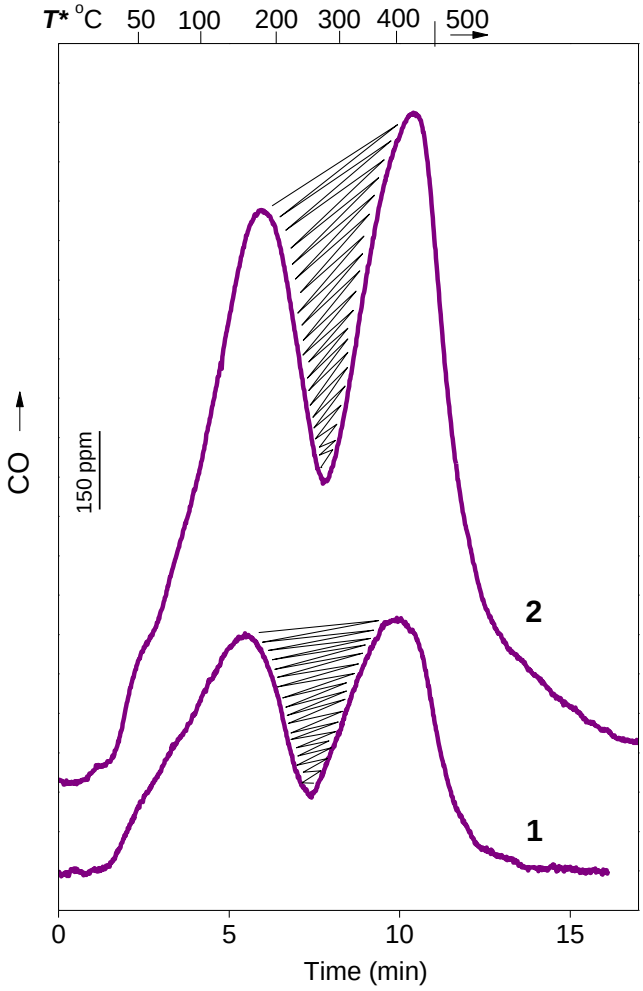

Fig. S31. CO TPD from fresh Pt/γ-Al_2O_3 samples after degassing and CO chemisorption. Pt loading 0.5 wt% (1) and 2.5 wt% (2); sample mass 400 mg (1) and 200 mg (2). During TPD runs, CO_2 was trapped at 77 K.

Note that the mass of 2.5%Pt/γ-Al_2O_3 sample is twice as small as that of 0.5%Pt/γ-Al_2O_3 but the dip in CO desorption rate is larger, in proportion to the amount of Pt (10 and 25 μmol in cases 1 and 2, respectively), not to the amount of the support. The area of the hatched fragments corresponds to 0.7 (1) and 1.5 (2) μmol CO.

Sample	CO_{ads}/Pt	CO_{ads} μmol	CO_{des} μmol	$CO_{2,des}$* μmol	CO_{des}+$CO_{2,des}$ μmol
1	0.75	7.6	3.8	3.6	7.4
2	0.68	17.3	11.5	5.7	17.2

*As measured after accumulating in the trap at 77 K.

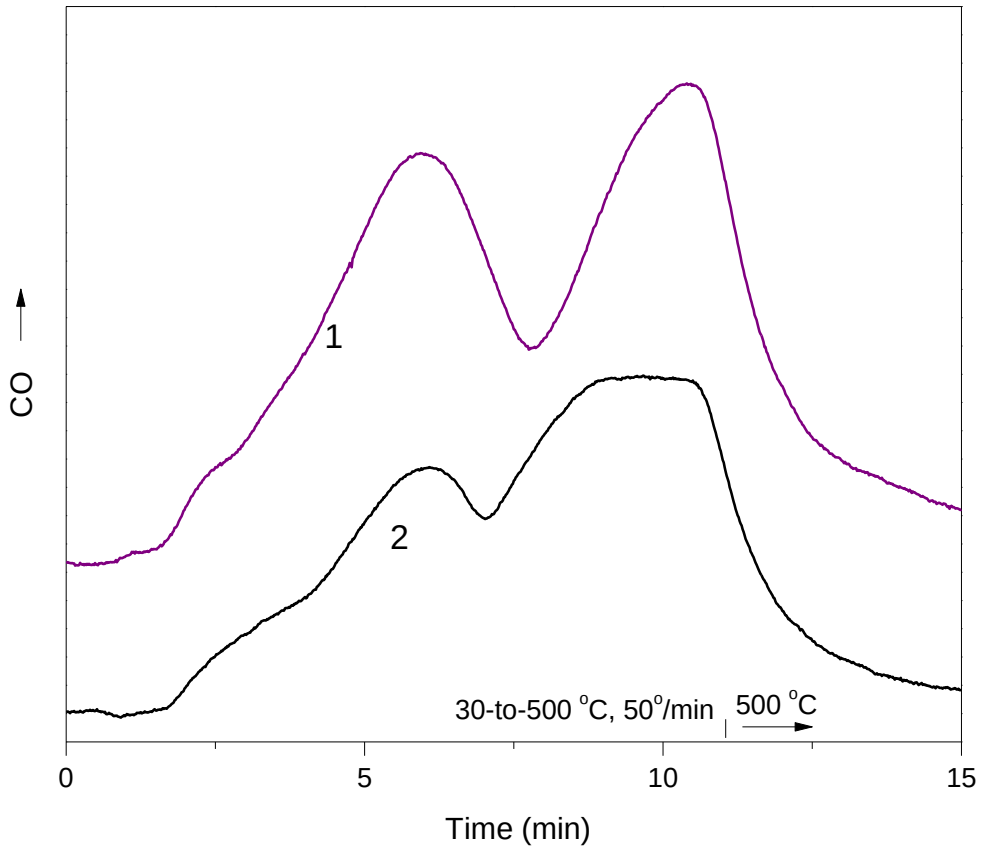

Fig. S32. CO TPD traces characteristic of fresh (1) and aged (2) 2.5%Pt/γ-Al_2O_3 sample, after degassing and CO chemisorption. Sample mass 200 mg: sample (2) was previously used in a few series of experiments, including storage in air, reoxidation, and rereduction.

The Table below lists corresponding CO/CO_2 adsorption/desorption values. Note that the CO_{ads}/Pt value for the aged sample is still rather high, corresponding to ~2 nm hemispherical Pt particles.

Sample	CO_{ads}/Pt	CO_{ads} µmol	CO_{des} µmol	$CO_{2,des}$* µmol	CO_{des}+$CO_{2,des}$ µmol
Fresh (1)	0.68	18.2	11.5	5.7	17.2
Aged (2)	0.52	13.7	7.3	4.6	11.9

*As measured after accumulating CO_2 in the trap at 77 K.

References

S1 O. A. Yakovina and A. S. Lisitsyn, Probing the H_2-induced restructuring of Pt nanoclusters by H_2-TPD, *Langmuir*, 2016, **32**, 12013–12021.

S2 A. S. Lisitsyn and O. A. Yakovina, On the origin of high-temperature phenomena in Pt/Al_2O_3. *Phys. Chem. Chem. Phys.*, 2018, **20**, 2339–2350.

S3 R. S. Hansen, R. R. Frost and J. A. Murphy, The thermal conductivity of hydrogen-helium mixtures. *J. Phys. Chem.*, 1964, **68**, 2028–2029.

S4 G. Castello, E. Biagini and S. Munari, The quantitative determination of hydrogen in gases, by gas chromatography with helium as the carrier gas. *J. Chromatogr. A*, 1965, **20**, 447–451.